Chapter 2

Interaction Coefficients for a Leaf Canopy

Myneni et al.

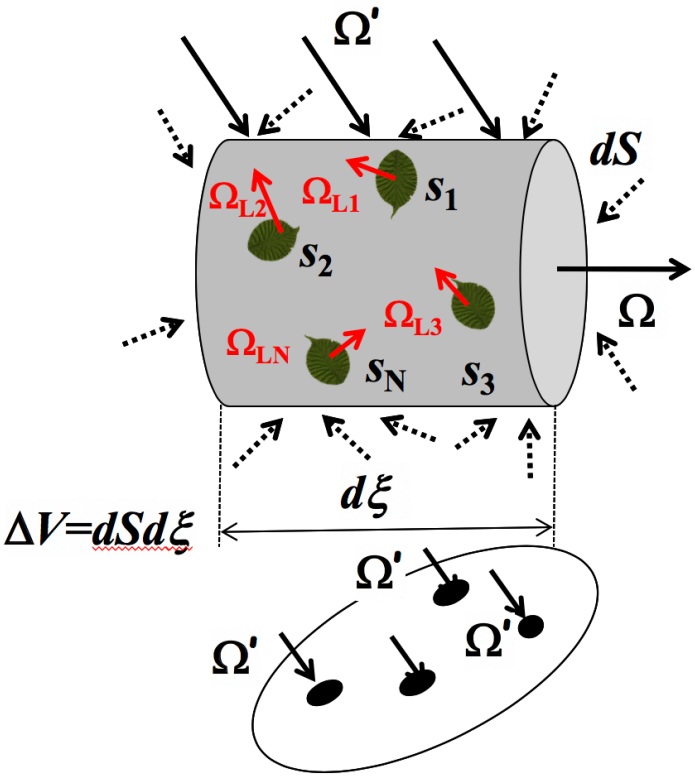

Chapter 2

Interaction Coefficients for a Leaf Canopy

1. Vegetation Canopy Structure

Turbid Medium Approximation: The vegetation canopy is idealized as a medium filled densely with small planar elements of negligible thickness and area, i.e., a turbid medium. All organs other than green leaves are ignored for the time being. Two important structural attributes – leaf area density and leaf normal orientation distribution – are first defined in order to quantify vegetation-photon interactions.

Leaf Area Density Distribution: The one-sided green leaf area per unit volume in the vegetation canopy is defined as the leaf area density distribution $u_L(\underline{r})$ (m^{-1}). The quantity,

$$L(x,y) = \int_0^{z_H} dz\, u_L(x,y,z), \tag{1}$$

is called the leaf area index, one-sided green leaf area per unit ground area at (x,y). Here Z_H is depth of the vegetation canopy. The vertical distribution of $\bar{u}_L(z)$,

$$\bar{u}_L(z) = \frac{1}{X_S Y_S} \int_0^{X_S} dx \int_0^{Y_S} dy\, u_L(x,y,z),$$

where X_S and Y_S are horizontal dimensions of a stand, shows the profile of leaf area distribution along the vertical. The variables L and $\bar{u}_L(z)$ are key parameters of climate, hydrology, bio-geochemistry and ecology models as they govern the exchange of energy, mass and momentum between the land surface and the atmospheric planetary boundary layer.

Direct measurements of L and $\bar{u}_L(z)$ are labor-intensive and expensive. The modeling of $u_L(\underline{r})$ is a challenge as it requires computer simulation of vegetation canopies based on tedious field

measurements (Fig. 1). Hence the interest in remote sensing of these variables from space-based measurements of reflected solar radiation and lidar backscatter returns (Fig. 2).

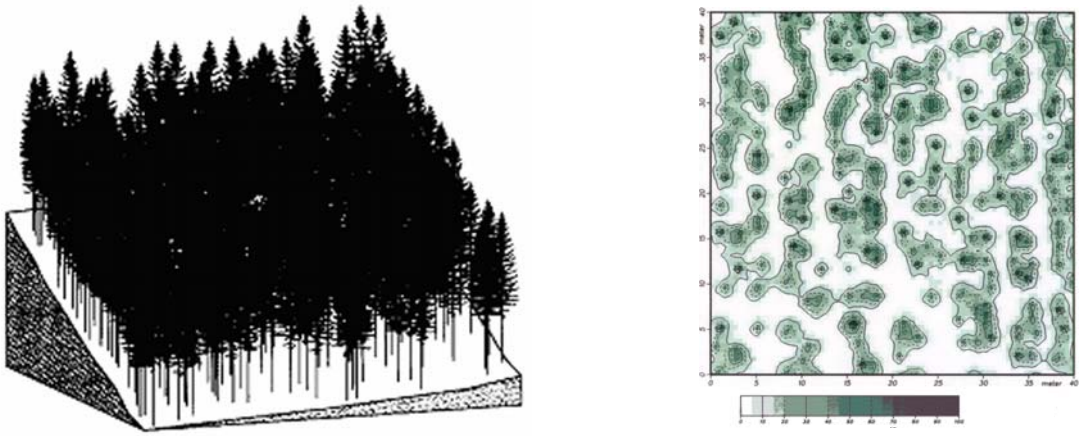

Figure 1. Computer simulated Norway spruce stand about 50 km near Goettingen, Germany, in the Harz mountains. The stand is about 45 years old and situated on the south slope. A 40×40 m^2 section of the stand with 297 trees was sampled for reconstruction. The stem diameters varied from 6 to 28 m and the tallest trees were about 12.5 m in height. The trees were divided into five groups with respect to stem diameter. A model of a Norway spruce based on fractal theory was used to build a representative of each group [Knyazikhin et al., 1996]. Given the distribution of tree stems in the stand, the diameter of each tree, the entire sample site was generated (left panel). The right panel shows the spatial distribution of leaf area index L(x,y) at spatial resolution of 50 cm^2, i.e., distribution of the mean leaf area index L(x,y) taken over each of 50 by 50 cm ground cells.

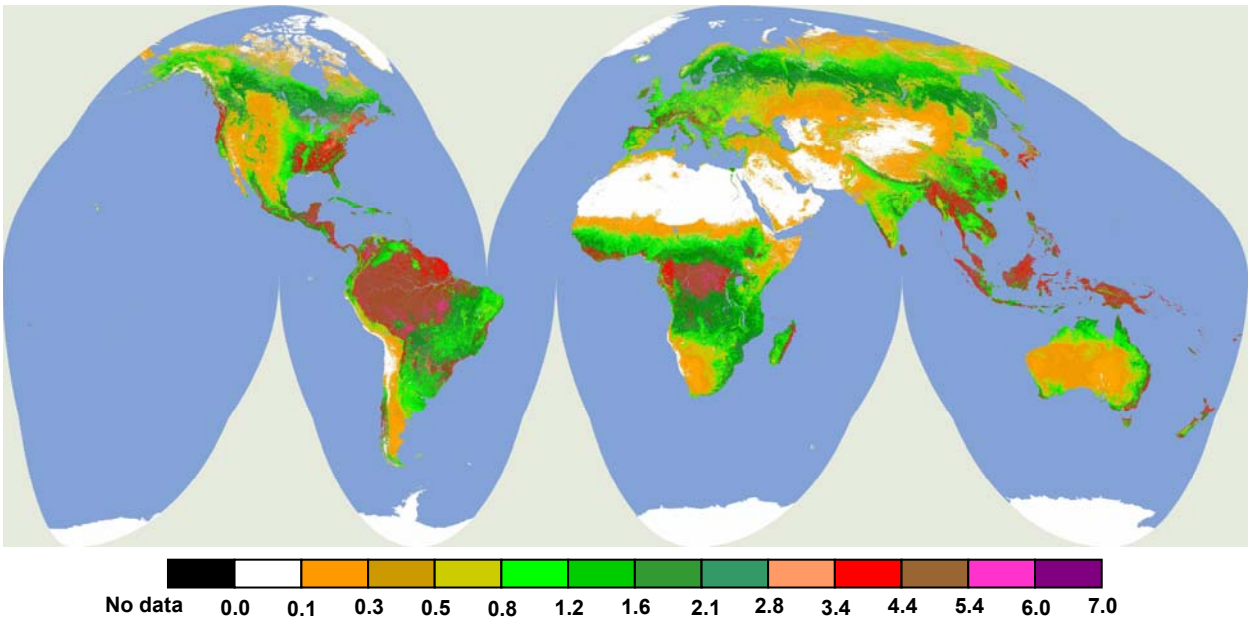

Figure 2. Global distribution of annual average vegetation green leaf area index L(x,y) at 1 km resolution derived from MODIS measurements of surface reflectances [Knyazikhin et al., 1998]. Data from a four year period, July 2000 to June 2004, were used to produce this image. This MODIS product has been developed from an algorithm based on radiative transfer theory developed in this book.

Needle Area Density Distribution: For non-flat leaves such as conifer needles, the counterpart to one-sided leaf area is the hemi-surface or half-of-total leaf (needle) area. In coniferous canopies, thus, the hemi-surface needle area is used in expressing the leaf area density (u_L) and leaf area index (LAI).

Leaf Normal Orientation Distribution: Let

$$\underline{\Omega}_L \equiv (\theta_L, \varphi_L) \equiv (\mu_L, \varphi_L), \quad \mu_L \in (0,1), \quad \varphi_L \in (0,2\pi)$$

be the normal to the upper face of a leaf element. If this normal is in the lower hemisphere, the lower face may be treated as the upper face, i.e., the definition of the upper face of a leaf element is the face the normal to which is in the upper hemisphere. Hence, the space of leaf normal orientation is always 2π steradians. Further, let $(1/2\pi)\, g_L(\underline{\Omega}_L)$ be the probability density function of leaf normal orientation,

$$\frac{1}{2\pi} \int_{2\pi+} d\underline{\Omega}_L \; g_L(\underline{\Omega}_L) = 1. \tag{2}$$

If μ_L and φ_L are assumed independent, then

$$\frac{1}{2\pi}\, g_L(\underline{\Omega}_L) = \bar{g}_L(\mu_L)\, \frac{1}{2\pi}\, h_L(\varphi_L), \tag{3}$$

where $\bar{g}_L(\mu_L)$ and $(1/2\pi)\, h_L(\varphi_L)$ are the probability density functions of leaf normal inclination and azimuth, respectively, and

$$\int_0^1 d\mu_L \, \bar{g}_L(\mu_L) = 1, \quad \frac{1}{2\pi} \int_0^{2\pi} d\varphi_L h_L(\varphi_L) = 1.$$

The functions $g_L(\underline{\Omega}_L)$, $\bar{g}_L(\mu_L)$ and $h_L(\varphi_L)$ will depend on the location $\underline{r}$ in the vegetation canopy but this has been suppressed for clarity.

The simplest model of leaf normal orientation distribution is constant leaf normal inclination and uniform distribution of azimuths,

$$\frac{1}{2\pi}\, g_L(\underline{\Omega}_L) = \frac{1}{2\pi} \delta(\mu_L - \mu_L^*). \tag{4}$$

The following example model distribution functions for leaf normal inclination are widely used [Bunnik, 1978]: (1) planophile – mostly horizontal leaves, (2) erectophile – mostly erect leaves, (3) plagiophile – mostly leaves at 45 degrees, (4) extremophile – mostly horizontal and vertical leaves, (5) uniform – all inclinations equally probable, and (6) spherical – leaf normals distributed as on a sphere. These distributions can be expressed as,

$$\text{Planophile:} \quad \bar{g}_L(\theta_L)\sin\theta_L = \frac{2}{\pi}(1+\cos 2\theta_L), \tag{5a}$$

$$\text{Erectophile:} \quad \bar{g}_L(\theta_L)\sin\theta_L = \frac{2}{\pi}(1-\cos 2\theta_L), \tag{5b}$$

$$\text{Plagiophile:} \quad \bar{g}_L(\theta_L)\sin\theta_L = \frac{2}{\pi}(1-\cos 4\theta_L), \tag{5c}$$

$$\text{Extremophile:} \quad \bar{g}_L(\theta_L)\sin\theta_L = \frac{2}{\pi}(1+\cos 4\theta_L), \tag{5d}$$

$$\text{Uniform:} \quad \bar{g}_L(\theta_L)\sin\theta_L = \frac{2}{\pi}, \tag{5e}$$

$$\text{Spherical:} \quad \bar{g}_L(\theta_L)\sin\theta_L = \sin\theta_L, \tag{5f}$$

and are plotted in Fig. 3.

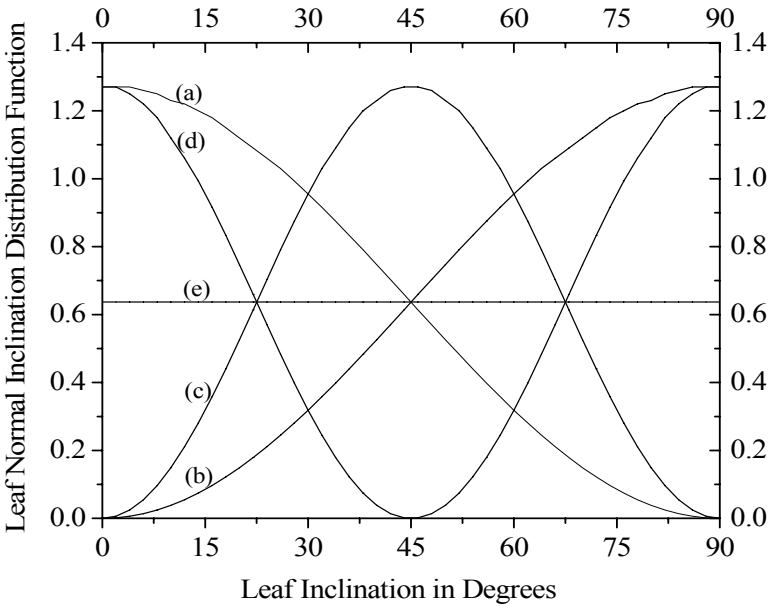

Figure 3. The $\bar{g}(\theta_L)\sin\theta_L$ for (a) planophile (mostly horizontall leaves), (b) erectorphile (mostly vertical leaves), (c) pla-giophile (leaves inclined mostly at about 45^0), (d) extremephile (mostly horizontal and vertical leaves) and (e) uniform (all inclina-tions equally probable) distributions.

Certain plants, such as soybeans and sunflowers, exhibit heliotropism, where the leaf azimuths have a preferred orientation with respect to the solar azimuth. A simple model for h_L in such canopies is [Verstraete, 1987],

$$\frac{1}{2\pi}h_L(\varphi_L,\varphi) = \frac{1}{\pi}\cos^2(\varphi-\varphi_L-\eta), \tag{6}$$

where η is the difference between the azimuth of the maximum of the distribution function h_L and the azimuth of the incident photon φ. In the case of diaheliotropic distributions, which tend to maximize the projected leaf area to the incident stream $\eta = 0$. On the other hand, paraheliotropic distributions tens to minimize the leaf area projected to the incident stream, $\eta = 0.5\pi$. A more general model for the leaf normal orientations is the beta distribution, the

parameters of which can be obtained from fits to field measurements of the leaf normal orientation [Goel and Strebel, 1984].

Needle and shoot orientation: The orientation of three-dimensional and non-cylindrical conifer needles however cannot be defined by one vector alone (as the leaf normal in case of flat leaves) but an additional vector is needed. These two vectors can be defined, for example, as the main axis of a needle and a normal to this axis (Oker-Blom and Kellomäki 1982). The needle axis defines the needle inclination for which the same characterizations as for planar leaves (e.g. a planophile or an erectophile needle inclination distribution) can be used. Whenever the needles are not cylindrical, the rotation angle, defined by the normal to the needle axis, must in addition be specified. We define the spherical needle orientation so that the needle main axis has no preferred direction in space and, for any fixed direction of the needle axis, the rotation angle is uniformly distributed.

Conifer needles are typically tightly grouped into annual shoots, which (for reasons that will become clear later) are often used as the basic foliage elements in modeling radiative transfer in coniferous canopies. To define shoot orientation, the same approach as defined above can be used (Stenberg 1996). For example, the main shoot axis has equal probability of pointing in any direction in the case of spherical shoot orientation distribution.

The shoot inclination in many conifer species changes with depth in the canopy so that it becomes more horizontal deeper down in the canopy. In shade-tolerant species, especially, this change is accompanied by changes in the shoot structure so that, for example, shade shoots are flatter than 'sun shoots' (Fig. 4).

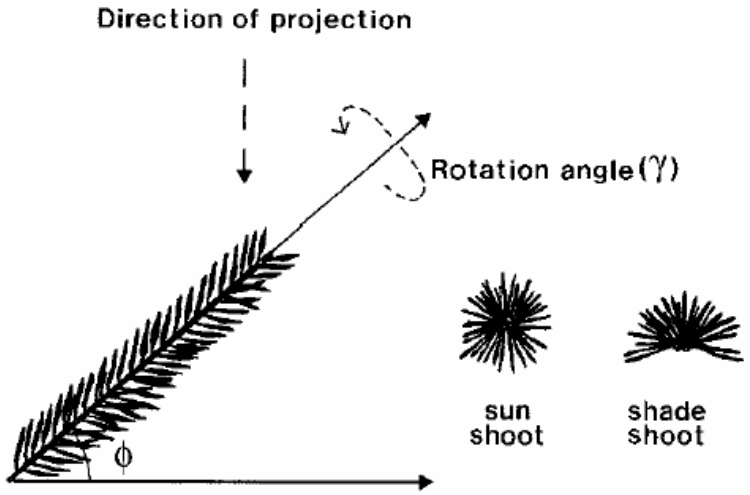

Figure 4. Determination of shoot orientation and illustration of 'sun shoot' and 'shade shoot' geometry.

2. Vegetation Canopy Optics

A photon incident on a leaf element can either be absorbed or scattered depending on its frequency. If the scattered photon emerges from the same side of the leaf as the incident photon, the event is termed reflection. Likewise, if the scattered photon exits the leaf from the opposite

side, the event is termed transmission. Scattering of solar radiation by green leaves does not involve frequency shifting interactions, but is dependent on the wavelength.

A photon incident on a leaf element can either be specularly reflected from the surface depending on its roughness or emerge diffused from interactions in the leaf interior. Some leaves can be quite smooth from a coat of wax-like material, while other leaves can have hairs making the surface rough. Light reflected from the leaf surface can be polarized as well. Specularly reflected photons contain no information about the constitution of the leaf material as this is a surface phenomenon. Photons that do not suffer surface reflection enter the interior of the leaf, where they are either absorbed or refracted because of the many refractive index discontinuities between the cell walls and intervening air cavities. Photons that are not absorbed in the interior of the leaf emerge on both sides, generally diffused in all directions.

Leaf Optics: The interaction of the electromagnetic radiation with plant leaves (reflection, transmission, absorption) depends on the chemical and physical characteristics of these leaves. The absorption is essentially a function of changes in the spin and angular momentum of electrons, transitions between orbital states of electrons in particular atoms (visible: chlorophylls 'a' and 'b', carotenoids, brown pigments, and other accessory pigments) and vibrational-rotational modes within the polyatomic molecules (near infrared and middle infrared: water). The refractive index discontinueties within the leaf ($n \approx 1.40$ for hydrated cell walls, $n \approx 1.33$ for water at 1 μm, and $n = 1$ for air) induce scattering.

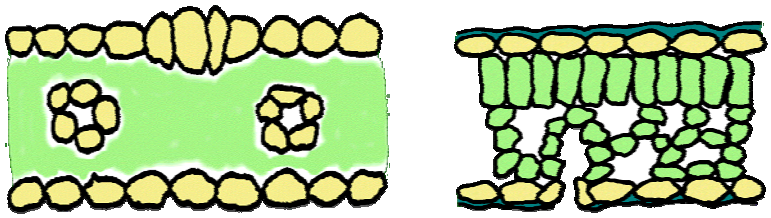

Figure 5. Schematic representation of Monocot (left) and Dicot (right) leaves. Leaf surface (epidermis) is shown in yellow, internal cells (mesophyll) are in green, and mist air space is in white.

Allen et al. (1969) has developed one early model of the leaf optical properties, called 'plate model'. The model considers a compact plant leaf as a single semi-transparent plate with plane parallel surfaces, illuminated by partially isotropic light. The expression for the total reflectance of the plate was derived by summing the amplitudes of successive reflections and refractions. However, plant leaves are not compact but present a wide range of anatomical structures which depend on the species (Fig. 5), which significantly limits the applicability of the 'plate model'. Jacquemoud and Baret (1990) have implemented the 'PROSPECT' model, one of the most popular 'generalized plate model' today. In this model a leaf is represented by a pile of N homogeneous layers separated by N-1 air spaces. The model considers surface layer and remaining N-1 internal layers separately to account for the fact that only surface layer may be exposed to non-isotropic radiation, while internal layers interact with the scattered radiation only. The process of refraction in the system of 1 and N-1 layers of the PROSPECT model is shown in Fig. 6a. An example of simulated leaf transmittance as a function of the spread of incidence angle of the incoming beam is shown in Fig. 6b.

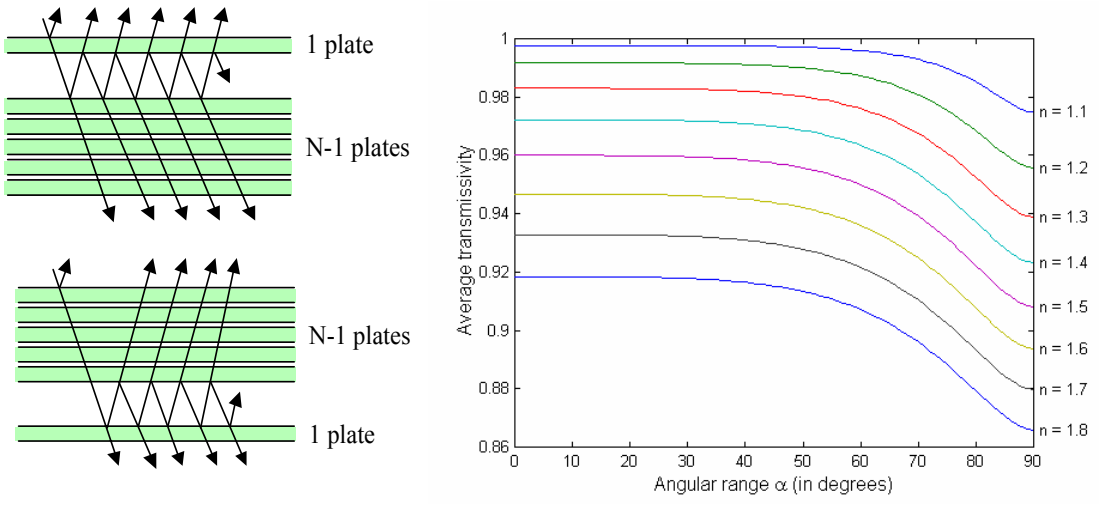

Figure 6. Modeling of leaf optics with the PROPSPECT model. The left panel shows the model representation of the leaf as a pile of N plates (1 surface plate and N-1 internal plates). The right panel shows the PROSPECT model simulations of leaf transmittance as a function of the spread of incidence angle of the incoming beam. Here $\alpha = 0$ corresponds to a monodirectional beam, while $\alpha = 90$ corresponds to a hemispherical flux.

Overall, the 'PROSPECT' model simulates the hemispherical reflectance and transmittance of various plant leaves (monocots, dicots or senescent leaves) over the solar spectrum (from 400 nm to 2500 nm). Scattering is described by a spectral refractive index (n) and a structure parameter, specifying the average number of air/cell wall interfaces within mesophyll (N). Absorption is modeled using pigment concentration (C_{a+b}, $\mu g\ cm^{-2}$), water content (C_w, cm or $g\ cm^{-2}$), and the corresponding specific spectral absorption coefficients (K_{a+b} and K_w). The internal parameters of the model (n, K_{a+b} and K_w) were estimated with field measurements (LOPEX data base for leaves, needles, stems, etc.) The remaining three key parameters (N, C_{a+b}, C_w) constitute the model's input to be adjusted for particular leaves types.

Leaf Scattering Phase Function: The angular distribution of radiant energy scattered by a leaf element is specified by the leaf element scattering phase function. Consider an elemental leaf area $d\sigma_L$ on which monochromatic radiation of intensity I is incident along $\underline{\Omega}'$. The amount of radiant energy flowing through the leaf area $d\sigma_L$ along $\underline{\Omega}'$ confined to the solid angle $d\underline{\Omega}'$ in a time interval dt is

$$d\,E' = I(\underline{\Omega}')\left|\underline{\Omega}_L \bullet \underline{\Omega}'\right| d\sigma_L d\underline{\Omega}' dt.$$

The wavelength dependence is assumed and will not be explicitly denoted in what follows. One part of $d\,E'$ is absorbed and the rest is scattered in all directions. Consider the direction $\underline{\Omega}$ about the solid angle $d\underline{\Omega}$ into which some part of the incident energy is scattered $d\,E$ upon interaction with the leaf element. The leaf scattering phase function γ_L which introduces the appropriate stream is

$$\gamma_L(\underline{\Omega}' \to \underline{\Omega}, \underline{\Omega}_L)d\underline{\Omega} = \frac{dE}{dE'}.$$

The leaf albedo, $\omega_L(\underline{\Omega}', \underline{\Omega}_L)$, is the fraction of incident energy scattered by the leaf, i.e.,

$$\omega_L(\underline{\Omega}', \underline{\Omega}_L) = \frac{\int_{4\pi} dE d\underline{\Omega}}{dE'} = \int_0^{2\pi} d\varphi \int_{-1}^{1} d\mu\, \gamma_L(\underline{\Omega}' \to \underline{\Omega}, \underline{\Omega}_L).$$

Radiant energy may be incident on the upper or the lower faces of the leaf element (–or +) and the scattering event may be either reflection or transmission. Integration of the leaf scattering phase function over the appropriate solid angles gives the leaf hemispherical reflectance $\rho_L^{\mp}$ and transmittance $\tau_L^{\mp}$ coefficients:

$$\rho_L^-(\underline{\Omega}', \underline{\Omega}_L) = \int_{(\underline{\Omega} \bullet \underline{\Omega}_L) > 0} \gamma_L(\underline{\Omega}' \to \underline{\Omega}, \underline{\Omega}_L)\, d\underline{\Omega}, \quad (\underline{\Omega}' \bullet \underline{\Omega}_L) < 0, \tag{7a}$$

$$\tau_L^-(\underline{\Omega}', \underline{\Omega}_L) = \int_{(\underline{\Omega} \bullet \underline{\Omega}_L) < 0} \gamma_L(\underline{\Omega}' \to \underline{\Omega}, \underline{\Omega}_L)\, d\underline{\Omega}, \quad (\underline{\Omega}' \bullet \underline{\Omega}_L) < 0, \tag{7b}$$

$$\rho_L^+(\underline{\Omega}', \underline{\Omega}_L) = \int_{(\underline{\Omega} \bullet \underline{\Omega}_L) < 0} \gamma_L(\underline{\Omega}' \to \underline{\Omega}, \underline{\Omega}_L)\, d\underline{\Omega}, \quad (\underline{\Omega}' \bullet \underline{\Omega}_L) > 0, \tag{7c}$$

$$\tau_L^+(\underline{\Omega}', \underline{\Omega}_L) = \int_{(\underline{\Omega} \bullet \underline{\Omega}_L) > 0} \gamma_L(\underline{\Omega}' \to \underline{\Omega}, \underline{\Omega}_L)\, d\underline{\Omega}, \quad (\underline{\Omega}' \bullet \underline{\Omega}_L) < 0. \tag{7d}$$

The leaf albedo $\omega_L(\underline{\Omega}', \underline{\Omega}_L)$ is simply the sum of ρ_L and τ_L; for example,

$$\omega_L(\underline{\Omega}', \underline{\Omega}_L) = \begin{cases} \rho_L^-(\underline{\Omega}', \underline{\Omega}_L) + \tau_L^-(\underline{\Omega}', \underline{\Omega}_L), & \text{if } (\underline{\Omega} \bullet \underline{\Omega}_L) < 0; \\ \rho_L^+(\underline{\Omega}', \underline{\Omega}_L) + \tau_L^+(\underline{\Omega}', \underline{\Omega}_L), & \text{if } (\underline{\Omega} \bullet \underline{\Omega}_L) > 0; \end{cases} \tag{8}$$

and in general depends on the incident photon direction $\underline{\Omega}'$ and the leaf normal orientation $\underline{\Omega}_L$. Typical spectra of a green leaf reflectance ρ_L and transmittance τ_L are shown in Fig. 7. The diffuse and specular leaf scattering phase functions are discussed below.

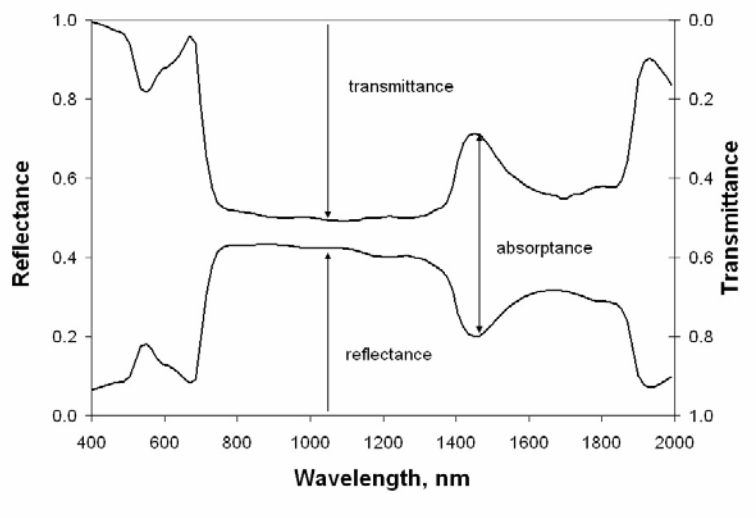

Figure 7. Typical reflectance (left axis) and transmittance (left axis) spectra of an individual plant leaf from 400 to 2000 nm for normal incidence. Note the following features – strong absorption at blue and red, moderate scattering at green, very strong scattering at near-infrared wavelengths and water absorption peaks in the mid-infra red. The dramatic increase in scattering from red (about 700 nm) to near-infrared (800-1100 nm) is often the basis for remote sensing of green vegetation.

Diffuse Leaf Scattering Phase Function: A simple but realistic model for diffuse leaf scattering phase function was proposed by Ross [1981] and others, and is extensively used in remote sensing works. In this model, a fraction $\rho_{L,d}$ of incident energy is assumed reflected in a cosine distribution (i.e., Lambertian) about the leaf normal. Similarly, another fraction $\tau_{L,d}$ is assumed transmitted in a cosine distribution on the opposite side of the leaf. In this model, transmission and reflection do not depend on whether radiant energy is incident on the upper or the lower side of the leaf element. This bi-Lambertian model can be written as

$$\gamma_{L,d}(\underline{\Omega}' \to \underline{\Omega}, \underline{\Omega}_L) = \begin{cases} \frac{1}{\pi}\rho_{L,d}\left|\underline{\Omega} \bullet \underline{\Omega}_L\right|, & (\underline{\Omega} \bullet \underline{\Omega}_L)(\underline{\Omega}' \bullet \underline{\Omega}_L) < 0, \\ \frac{1}{\pi}\tau_{L,d}\left|\underline{\Omega} \bullet \underline{\Omega}_L\right|, & (\underline{\Omega} \bullet \underline{\Omega}_L)(\underline{\Omega}' \bullet \underline{\Omega}_L) > 0. \end{cases} \tag{9}$$

Specular Leaf Scattering Phase Function*:* Specular reflection from the leaf surface depends on the angle of incidence α' (the angle between the leaf normal $\underline{\Omega}_L$ and the incident photon direction $\underline{\Omega}$, the wax coat refractive index n and the roughness of the leaf surface κ. The index of refraction n is a weak function of wavelength and a standard value of about 0.9 is used in most studies (which is why specularly reflected light from smooth leaves looks white). A simple model for specular leaf scattering phase function $\gamma_{L,S}$ is

$$\gamma_{L,S}(\underline{\Omega}' \to \underline{\Omega}, \underline{\Omega}_L) = F_r(n, \alpha')\, K(\kappa, \alpha')\, \delta_2(\underline{\Omega} \bullet \underline{\Omega}^*). \tag{10}$$

Here, F_r is the Fresnel reflectance averaged over the polarization states,

$$F(n, \alpha') = \frac{1}{2}\left[\frac{\sin^2(\alpha' - \theta_s)}{\sin^2(\alpha' + \theta_s)} + \frac{\tan^2(\alpha' - \theta_s)}{\tan^2(\alpha' + \theta_s)}\right],$$

where $\sin\theta_s = (\sin\alpha')/n$. The function K defines the correction factor for Fresnel reflection ($0 \le K \le 1$), and the argument $\kappa \approx 0.1$ to 0.3 characterizes the roughness of the surface. A simple model for leaf surface roughness is

$$K(k, \alpha') = \exp\left[-\kappa \tan(|\alpha'|)\right].$$

The function δ_2 is a surface delta function,

$$\delta_2(\underline{\Omega}, \underline{\Omega}^*) = 0, \qquad \underline{\Omega} \neq \underline{\Omega}^*, \quad \int_{4\pi} d\underline{\Omega}\, q(\underline{\Omega})\, \delta_2(\underline{\Omega} \bullet \underline{\Omega}^*) = q(\underline{\Omega}^*). \tag{11}$$

The vector $\underline{\Omega}^* = \underline{\Omega}^*(\underline{\Omega}, \underline{\Omega}_L)$ defines the direction of specular reflection. The leaf albedo for specular reflection is therefore,

$$\int_{4\pi} d\underline{\Omega}\, \gamma_{L,s}(\underline{\Omega}' \to \underline{\Omega}, \underline{\Omega}_L) = \omega_{L,s}(\alpha', n, \kappa) = K(\kappa, \alpha')\, F_r(n, \alpha'). \tag{12}$$

3. Total Interaction Coefficient

The probability that a photon while traveling a distance $d\xi$ in the medium will interact with the elements of the host medium is given by $\sigma(\underline{r}, \underline{\Omega})d\xi$ where $\sigma(\underline{r}, \underline{\Omega})$ is the total interaction coefficient (m^{-1}). This probability can be derived as follows.

Consider an elementary volume $dSd\xi$ at r in the medium and which contains a sufficient number of small planar leaf elements of negligible thickness. The probability that photons in the incident radiation will collide with leaf elements in this volume is given by the ratio of the total shadow area of leaves on a plane perpendicular to the direction of photon travel $\underline{\Omega}$ to the area dS,

$$\sigma(\underline{r}, \underline{\Omega})d\xi \equiv \frac{\text{total shadow area on a plane perpendicular to } \underline{\Omega}}{dS}$$

$$= \frac{s_1 |\underline{\Omega}_{L1} \bullet \underline{\Omega}| + s_2 |\underline{\Omega}_{L2} \bullet \underline{\Omega}| + \ldots + s_N |\underline{\Omega}_{LN} \bullet \underline{\Omega}|}{dS}$$

where s_i is the area of leaf element of orientation $\underline{\Omega}_{Li}$. If the leaf elements are sufficiently small and numerous, their shadows do not overlap and, the ratio of the area of all leaf elements $\bar{s}_i$ of orientation $\underline{\Omega}_{Li}$ to the total leaf area S_o in the elementary volume is equivalent to the number or the probability of leaf elements of orientation $\underline{\Omega}_{Li}$, that is,

$$\bar{s}_i(\underline{\Omega}_{Li})/S_o = (1/2\pi) g_L(\underline{r}, \underline{\Omega}_{Li}) d\underline{\Omega}_{Li}.$$

Thus,

$$\sigma(\underline{r},\underline{\Omega})d\xi = \frac{S_o}{dS}\left[\frac{1}{2\pi}g_L(\underline{r},\underline{\Omega}_{L1})d\underline{\Omega}_{L1}\,|\,\underline{\Omega}_{L1}\bullet\underline{\Omega}\,| + \frac{1}{2\pi}g_L(\underline{r},\underline{\Omega}_{L2})d\underline{\Omega}_{L2}\,|\,\underline{\Omega}_{L2}\bullet\underline{\Omega}\,| + ...\right]$$

$$= \frac{S_o}{dS}\frac{1}{2\pi}\int_{2\pi+} d\underline{\Omega}_L g_L(\underline{r},\underline{\Omega}_L)\,|\,\underline{\Omega}_L\bullet\underline{\Omega}\,|$$

$$= \frac{S_o}{dS}G(\underline{r},\underline{\Omega}_L).$$

Therefore,

$$\sigma(\underline{r},\underline{\Omega}) = u_L(\underline{r})G(\underline{r},\underline{\Omega}), \tag{13}$$

because $(S_o/dSd\xi)$ is the leaf area per unit volume or the leaf area density $u_L(\underline{r})$. The function $G(\underline{r},\underline{\Omega})$ is the geometry factor, first proposed by Ross [1981], and may be defined as the projection of unit leaf area at r onto a plane perpendicular to the direction of photon travel $\underline{\Omega}$. The geometry factor G satisfies the following condition:

$$\frac{1}{2\pi}\int_{2\pi+} d\underline{\Omega}\, G(\underline{r},\underline{\Omega}) = \frac{1}{2}. \tag{14}$$

Example G–functions for model leaf normal orientations are shown in Fig. 8.

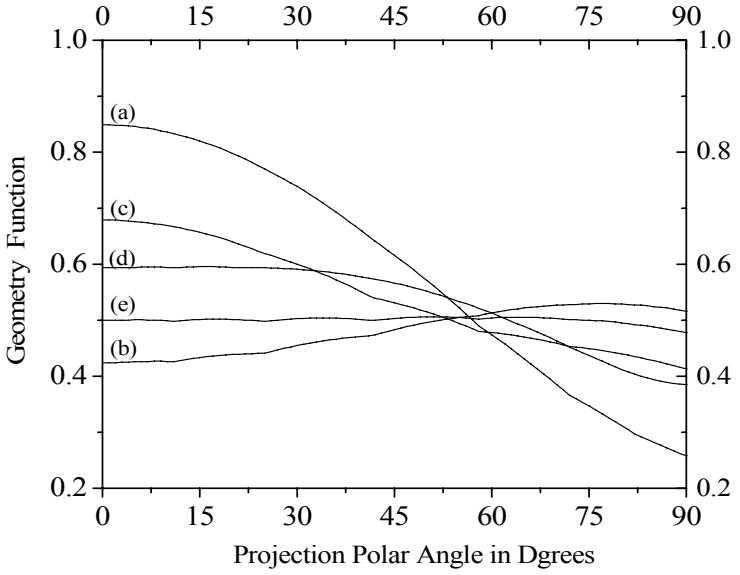

Figure 8. The G-function with projection zenith angle θ for (a) planophile, (b) erectophile, (c) plagiophile, (d) extremophile and (e) spherical leaf normal distribution functions. A distribution with mostly horizontal leaves (planophile) has a higher probability of intcercepting photons incident from directions close to the vertical and vice-versa. The G-function for uniform orientation is equal to one-half. Variations seen in the figure are due to numerical errors.

It is important to note that the geometry factor is an explicit function of the direction of photon travel Ω in the general case of non-uniformly distributed leaf normals. This imbues directional dependence to the interaction coefficients in the case of vegetation canopies, that is, the vegetation canopy radiation transport is non-rotationally invariant. The transport problem reduce to the classical rotationally invariant form only in the case of spherically distributed leaf normals (G = 0.5). Another noteworthy point is the frequency independence of σ, that is, the extinction

probabilities for photons in vegetation media are determined by the structure of the canopy rather than photon frequency or the optics of the canopy.
The total interaction coefficient $\sigma(\underline{r},\underline{\Omega})$ can be estimated from transmission measurements made below the vegetation canopy at wavelengths where leaves strongly absorb the incident radiation. Such measurements can be inverted to solve for the leaf area density distribution $u_L(\underline{r})$ and the leaf normal orientation distribution function $(1/2\pi)g_L(\underline{\Omega}_L)$.

The G-function for needles and shoots: The geometry factor G for needles varies with the cross-sectional needle shape, including forms close to a half circle (Scots pine) or a rhomb (Norway spruce), and cannot be calculated using the simple expressions (sf. Problem Sets, Problem 8). For vertical needles with uniform rotation angle, however, the same value $G = (2/\pi)\sin\theta$ as for vertical leaves is obtained (Oker-Blom and Kellomäki 1982). More importantly, the condition given by Eq. (14) that the mean of G over all possible directions equals 0.5 holds true also for needles, irrespective of their shape as long as they are convex (Lang 1991). Also, the G value of spherically oriented needles equals 0.5 for all directions of the incoming beam.

When using the coniferous shoot as the basic foliage element, the geometry factor G corresponds to the ratio of the shoot's silhouette area on a plane perpendicular to the direction of photon travel to the hemi-surface needle area. Oker-Blom and Smolander (1988) defined it as the silhouette to total area ratio (STAR), where the total (all-sided) needle area was used in the denominator. Because here we use the hemi-surface leaf area as the common basis for both flat leaves and needles, the shoot geometry factor G equals $2\times\mathrm{STAR}$.

The G value of spherically oriented shoots ($2\times\overline{\mathrm{STAR}}$) no longer equals 0.5 but is essentially smaller due to needle overlapping in the shoot (i.e. the shoot is not a convex object). Empirical data for Scots pine and Norway spruce shoots show a range of approximately 0.2 to 0.4 (smaller values in the upper canopy and higher values in lower canopy) and a mean around 0.3 for $2\times\overline{\mathrm{STAR}}$. This corresponds to a 40 % reduction in the G value of shoots as compared to that of single leaves or needles (for which G=0.5)

4. Differential Scattering Coefficient

The probability that a photon while traveling a distance $d\xi$ in the medium will scatter from direction $\underline{\Omega}'$ to direction $\underline{\Omega}$ is given by $\sigma_s(\underline{r},\underline{\Omega}'\rightarrow\underline{\Omega})d\underline{\Omega}\,d\xi$ where σ_s is the differential scattering coefficient (m^{-1} sr^{-1}). This probability can be derived as follows.

Consider an elementary volume $dSd\xi$ at r in the medium and which contains a sufficient number of small planar leaf elements of negligible thickness. The probability that photons incident along $\underline{\Omega}'$ will scatter into a differential solid angle about $\underline{\Omega}$ is given by

$$\sigma_s(\underline{r},\underline{\Omega}'\rightarrow\underline{\Omega})d\underline{\Omega}\,d\xi = \frac{s_1\,|\,\underline{\Omega}_{L1}\bullet\underline{\Omega}'\,|\,\gamma_L(\underline{\Omega}_{L1};\underline{\Omega}'\rightarrow\underline{\Omega})d\underline{\Omega}}{dS}$$

$$+\frac{s_2\,|\,\underline{\Omega}_{L2}\bullet\underline{\Omega}'\,|\,\gamma_L(\underline{\Omega}_{L2};\underline{\Omega}'\rightarrow\underline{\Omega})d\underline{\Omega}}{dS}+\ldots+\frac{s_N\,|\,\underline{\Omega}_{LN}\bullet\underline{\Omega}'\,|\,\gamma_L(\underline{\Omega}_{LN};\underline{\Omega}'\rightarrow\underline{\Omega})d\underline{\Omega}}{dS},$$

where s_i is the area of leaf element of orientation $\underline{\Omega}_{Li}$ and γ_L is the scattering phase function. The point interactions are assumed to be independent and uncorrelated. Implicit in the formulation of the above is the assumption that the leaf elements are sufficiently small and numerous. The ratio of the area of all leaf elements $\bar{s}_i$ of orientation $\underline{\Omega}_{Li}$ to the total leaf area S_o in the elementary volume is therefore equivalent to the number or the probability of leaf elements of orientation $\underline{\Omega}_{Li}$, that is, $\bar{s}_i(\underline{\Omega}_{Li})/S_o = (1/2\pi)g_L(\underline{r},\underline{\Omega}_{Li})d\underline{\Omega}_{Li}$, and,

$$\begin{aligned}\sigma_s(\underline{r},\underline{\Omega}'\rightarrow\underline{\Omega})d\underline{\Omega}\,d\xi &= \frac{S_o}{dS}\Big[\frac{1}{2\pi}g_L(\underline{r},\underline{\Omega}_{L1})d\underline{\Omega}_{L1}\,|\,\underline{\Omega}_{L1}\bullet\underline{\Omega}'\,|\,\gamma_L(\underline{\Omega}_{L1};\underline{\Omega}'\rightarrow\underline{\Omega})d\underline{\Omega}\\ &\qquad +\frac{1}{2\pi}g_L(\underline{r},\underline{\Omega}_{L2})d\underline{\Omega}_{L2}\,|\,\underline{\Omega}_{L2}\bullet\Omega'\,|\,\gamma_L(\underline{\Omega}_{L2};\underline{\Omega}'\rightarrow\underline{\Omega})d\underline{\Omega}+..\Big]\\ &= \frac{S_o}{dS}d\underline{\Omega}\frac{1}{2\pi}\int_{2\pi+}d\underline{\Omega}_L g_L(\underline{r},\underline{\Omega}_L)\,|\,\underline{\Omega}_L\bullet\underline{\Omega}'\,|\,\gamma_L(\underline{\Omega}_L;\underline{\Omega}'\rightarrow\underline{\Omega})\\ &= \frac{S_o}{dS}d\underline{\Omega}\frac{1}{\pi}\Gamma(\underline{r},\underline{\Omega}'\rightarrow\underline{\Omega}).\end{aligned}$$

Thus the differential scattering coefficient may be written as,

$$\sigma_s(\underline{r},\underline{\Omega}'\rightarrow\underline{\Omega}) = u_L(\underline{r})\frac{1}{\pi}\Gamma(\underline{r},\underline{\Omega}'\rightarrow\underline{\Omega}), \tag{15}$$

because $(S_o/dSd\xi)$ is the leaf area per unit volume or the leaf area density $u_L(\underline{r})$. Here $(1/\pi)\Gamma$ is the area scattering phase function first proposed by Ross [1981]. It is important to note that the differential scattering coefficient is non-rotationally invariant, that is, it is an explicit function of the polar coordinates of $\underline{\Omega}'$ and $\underline{\Omega}$. It can be reduced to the rotationally invariant form, $\sigma_s(\underline{r},\underline{\Omega}'\rightarrow\underline{\Omega}) = \sigma_s(\underline{r},\underline{\Omega}'\bullet\underline{\Omega})$ in a few limited cases. This property precludes the use of Legendre polynomial expansion and the addition theorem typically used in transport theory for handling the scattering integral.

The scattering phase function combines diffuse scattering from the interior of a leaf and specular reflection from the leaf surface,

$$\Gamma(\underline{r},\underline{\Omega}'\rightarrow\underline{\Omega}) = \Gamma_d(\underline{r},\underline{\Omega}'\rightarrow\underline{\Omega})+\Gamma_s(\underline{r},\underline{\Omega}'\rightarrow\underline{\Omega}).$$

The functions Γ_d and Γ_s are discussed below.

Area Scattering Phase Function for Diffuse Scattering: With the bi-Lambertian leaf scattering phase function introduced earlier [Eq. (9)], the diffuse area scattering phase function $\Gamma_d(\underline{r},\underline{\Omega}' \to \underline{\Omega}) = \Gamma_d(\underline{r},\underline{\Omega} \to \underline{\Omega}')$ may be written as,

$$\Gamma_d(\underline{r},\underline{\Omega}' \to \underline{\Omega}) = \rho_{L,d}\Gamma_d^-(\underline{r},\underline{\Omega}' \to \underline{\Omega}) + \tau_{L,d}\Gamma_d^+(\underline{r},\underline{\Omega}' \to \underline{\Omega}), \tag{16}$$

where,

$$\Gamma_d^{\pm}(\underline{\Omega}' \to \underline{\Omega}) = \pm\frac{1}{2\pi}\int_0^1 d\mu_L \int_0^{2\pi} d\varphi_L \; g_L(\mu_L,\varphi_L)\,(\underline{\Omega}\bullet\underline{\Omega}_L)\,(\underline{\Omega}'\bullet\underline{\Omega}_L)\,. \tag{17}$$

The ($\pm$) in the above definition indicates that the φ_L integration is over that portion of the interval $[0,2\pi]$ for which the integrand is either positive (+) or negative (–). The dependence on spatial point r is suppressed for clarity. The bi-Lambertian phase function imbues the area scattering phase function with a useful symmetry property,

$$\Gamma_d(\underline{\Omega}' \to \underline{\Omega}) = \Gamma_d(\underline{\Omega} \to \underline{\Omega}') = \Gamma_d(-\underline{\Omega}' \to -\underline{\Omega}).$$

For the special case of $\rho_{L,d} = \tau_{L,d}$, an additional symmetry holds,

$$\Gamma_d(\underline{\Omega}' \to \underline{\Omega}) = \Gamma_d(-\underline{\Omega}' \to \underline{\Omega}).$$

An expression for the diffuse area scattering phase function can be derived from Eqs. (16) and (17) in canopies with horizontal, vertical and uniformly distributed leaf normals. For horizontal leaves $\mu_L = 1$, one obtains,

$$\Gamma_d(\underline{\Omega}' \to \underline{\Omega}) = \begin{cases} \tau_{L,d}\,\mu\mu', & \mu\mu' > 0, \\ \rho_{L,d}\,|\mu\mu'|, & \mu\mu' < 0. \end{cases} \tag{18}$$

For vertical leaf orientations ($\mu_L = 0$)

$$\Gamma_d(\underline{\Omega}' \to \underline{\Omega}) = \Gamma_1(\beta)\sqrt{1-\mu^2}\,\sqrt{1-\mu'^2}\,, \tag{19}$$

where $\beta \equiv \varphi - \varphi'$; $0 \le \beta \le 2\pi$, and,

$$\Gamma_1(\beta) = \frac{\omega_{L,d}}{2\pi}(\sin\beta - \beta\cos\beta) + \frac{\tau_{L,d}}{2}\cos\beta.$$

In the case of spherically distributed leaf normals, the rotationally invariant scattering phase function is

$$\Gamma_d(\underline{\Omega}' \to \underline{\Omega}) = \frac{\omega_L}{3\pi}(\sin\beta - \beta\cos\beta) + \frac{\tau_L}{\pi}\cos\beta, \tag{20}$$

where $\beta \equiv \arccos(\underline{\Omega}' \bullet \underline{\Omega})$. This form of Γ_d is illustrated in Fig. 9.

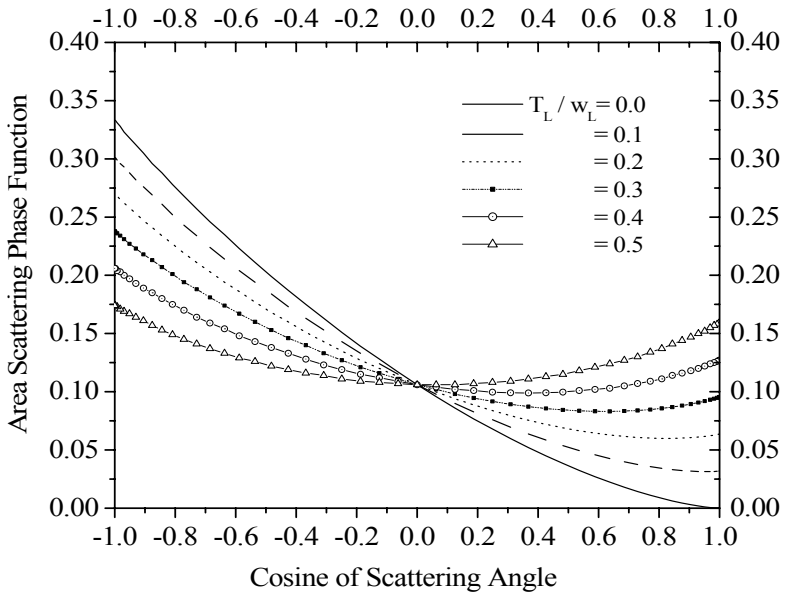

Figure 9. The area scattering phase function $\Gamma(\underline{\Omega}' \to \underline{\Omega})$ for uniformly distributed leaf normals. Each leaf is assumed to scatter according to the bi-Lambertian model. This function is rotationally invariant and in such cases the radiative transfer equation can be solved using standard methods developed in astrophysics and atmospheric physics.

In the general case of distributed leaf normals, the non-rotationally invariant form of the scattering kernel must be solved numerically [Eq. (17)]. Some simplifications are possible in the case of uniform distribution of leaf normal azimuths $h_L = 1$ and the bi-Lambertian leaf scattering phase function. This is achieved by azimuthal averaging of the scattering kernel,

$$\Gamma_d(\mu' \to \mu) = \frac{1}{2\pi}\int_0^{2\pi} d\varphi\, \Gamma_d(\underline{\Omega}' \to \underline{\Omega})$$

$$= \int_0^1 d\mu_L g_L(\mu_L)\left[\tau_{L,d}\Psi^+(\mu,\mu',\mu_L) + \rho_{L,d}\Psi^-(\mu,\mu',\mu_L)\right], \tag{21}$$

where

$$\Psi^{\pm}(\mu,\mu',\mu_L) = (\pm)\frac{1}{4\pi^2}\int_0^{2\pi} d\varphi \int_0^{2\pi} d\varphi_L (\underline{\Omega}' \bullet \underline{\Omega}_L)(\underline{\Omega} \bullet \underline{\Omega}_L). \tag{22}$$

The double integration over φ and φ_L for bi-Lambertian scattering distributions also eliminates φ'. Evaluation of the double integral in Eq. (22) gives [cf. Shultis and Myneni, 1988],

$$\Psi^{\pm}(\mu,\mu',\mu_L) = H(\mu,\mu_L)H(\pm\mu',\mu_L) + H(-\mu,\mu_L)H(\mp\mu',\mu_L), \tag{23}$$

where the H function is,

$$H(\mu,\mu_L)=\begin{cases}\mu\mu_L, & \text{if } (\cot\theta\cot\theta_L)>1,\\ 0, & \text{if } (\cot\theta\cot\theta_L)<-1,\\ \frac{1}{\pi}\left[\mu\mu_L\varphi_t(\mu)+\sqrt{1-\mu^2}\sqrt{1-\mu_L^2}\sin\varphi_t(\mu)\right], & \text{otherwise}\end{cases}$$

and,

$$\sin\varphi_t(\mu)=-\cot\theta\cot\theta_L=\pi-\varphi_t(-\mu).$$

The H function is shown in Fig. 10.

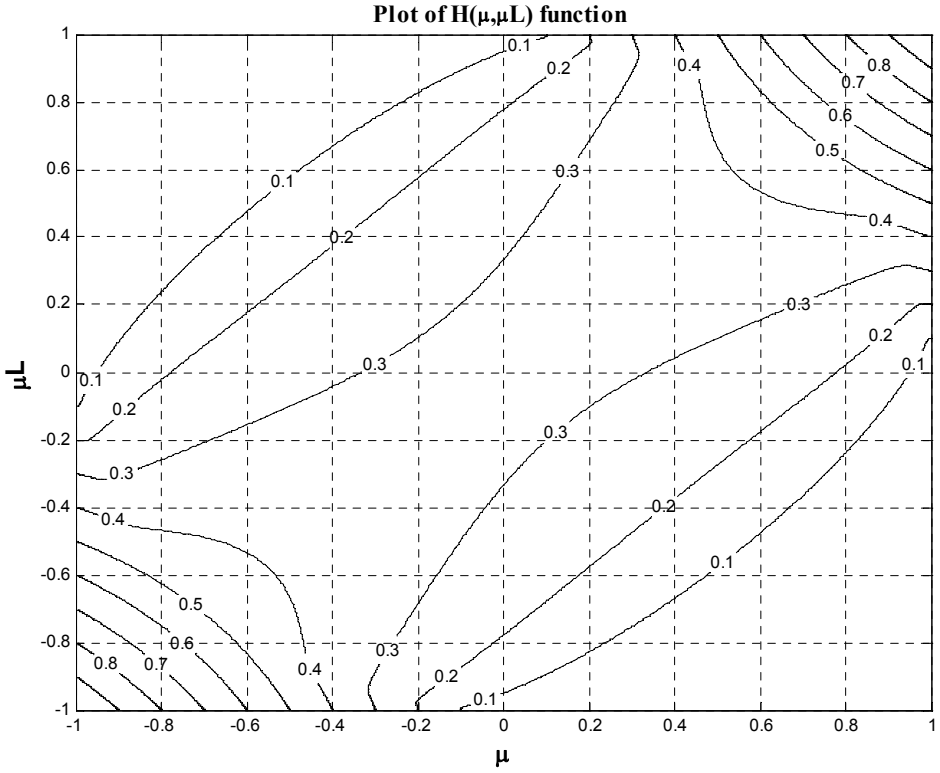

Figure 10. A contour plot of $H(\mu,\mu_L)$ function.

The azimuthally averaged area scattering phase function also possesses symmetry properties, namely,

$$\Gamma_d(\mu'\to\mu)=\Gamma_d(\mu\to\mu')=\Gamma_d(-\mu'\to-\mu).$$

For the special case of $\rho_{L,d}=\tau_{L,d}$, Eqs. (21) reduces to,

$$\Gamma_d(\mu' \to \mu) = \frac{\omega_{L,d}}{2}\int_0^1 d\mu_L g_L(\mu_L)\left[H(\mu,\mu_L) + H(-\mu,\mu_L)\right]\left[H(\mu',\mu_L) + H(-\mu',\mu_L)\right]$$

$$= \frac{\omega_{L,d}}{2}\int_0^1 d\mu_L g_L(\mu_L)\psi(\mu,\mu_L)\psi(\mu',\mu_L), \tag{24}$$

and an additional symmetry occurs, $\Gamma_d(\mu' \to \mu) = \Gamma_d(-\mu' \to -\mu)$. The function ψ in Eq. (24) is given in the Problem 8 of the Problems Sets Section). In the case of horizontal leaf orientation, the area scattering phase function is independent of exit azimuth [Eq. (18)]. However, in the case of vertical leaves, this is not so [Eq. (19)], and integration over φ from 0 to 2π or alternately over β from 0 to π results in,

$$\Gamma_d(\mu' \to \mu) = \frac{2\,\omega_{L,d}}{\pi^2}\sqrt{1-\mu^2}\sqrt{1-\mu'^2}. \tag{25}$$

The scattering coefficient for diffuse bi-Lambertian scattering from the leaf interior σ'_s has the explicit form [cf. Eq. (15), (10)],

$$\sigma'_s(\underline{r},\underline{\Omega}') = u_L(\underline{r})\frac{1}{\pi}\int_{4\pi} d\underline{\Omega}\,\Gamma_d(\underline{\Omega}' \to \underline{\Omega})$$

$$= u_L(\underline{r})\,\omega_{L,d}G(\underline{\Omega}'). \tag{26}$$

The normalized scattering phase function $(1/4\pi)P_d$ is therefore,

$$P_d(\underline{\Omega}' \to \underline{\Omega}) = \frac{4\Gamma_d(\underline{\Omega}' \to \underline{\Omega})}{\omega_{L,d}G(\underline{\Omega}')}, \tag{27}$$

such that,

$$\frac{1}{4\pi}\int_{4\pi} d\underline{\Omega}\,P_d(\underline{\Omega}' \to \underline{\Omega}) = 1.$$

The normalized scattering phase function $P_d(\underline{\Omega}' \to \underline{\Omega})$ for planophile leaf normal inclination distribution and bi-Lambertian leaf scattering distribution is shown in Fig. 11. It is clear that the scattering phase functions in leaf canopies are non-rotationally invariant, that is, they are not unique functions of $(\underline{\Omega}' \bullet \underline{\Omega})$.

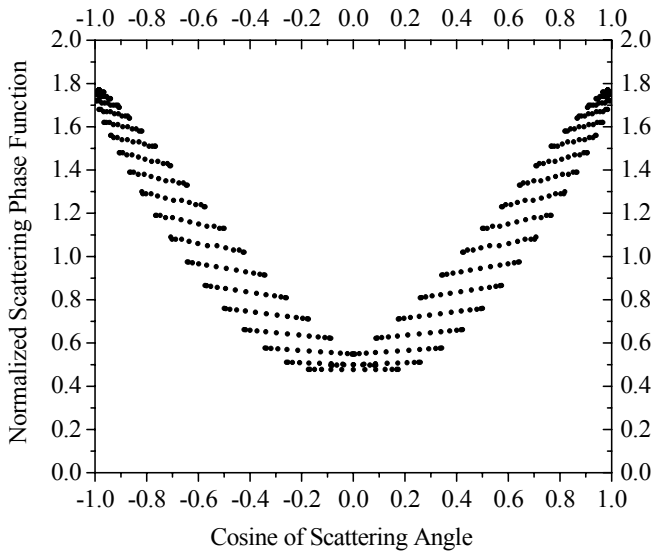

Figure 11. The normalized azimuthally dependent phase function $P(\underline{\Omega}' \rightarrow \underline{\Omega})$ for a planophile canopy [predominantly horizontal leaves]. The leaf transmittance and reflectance are both equal to 0.5, and $\underline{\Omega}'$ is fixed at $\theta' = 170^0$ and $\varphi = 0^0$. Each dot is the value of the phase function for a discrete value of $\Omega_{ij} = (\mu_i, \varphi_j)$ [the nearly horizontal row of dots is for a fixed μ_i and $, \varphi_j$ varies]. These results illustrate that the phase function is non rotationally invariant, i.e., it depends on the coordinates $\underline{\Omega}'$ and $\underline{\Omega}$ and not just on the scattering angle [acos $(\underline{\Omega} \bullet \underline{\Omega}')$].

Area Scattering Phase Function for Specular Reflection: Using the model described earlier [Eq. (10)] for specular reflection from leaf surfaces, the area scattering phase function for specular reflection can be evaluated as (cf. $d\underline{\Omega}_L = d\underline{\Omega}^*/4|\underline{\Omega}' \bullet \underline{\Omega}_L|$),

$$\begin{aligned}
\frac{1}{\pi}\Gamma_s(\underline{\Omega}' \rightarrow \underline{\Omega}) &= \frac{1}{2\pi}\int_{2\pi+} d\underline{\Omega}_L \; g_L(\underline{\Omega}_L)\,|\underline{\Omega}' \bullet \underline{\Omega}_L|\,\gamma_{L,s}(\underline{\Omega}' \rightarrow \underline{\Omega}, \underline{\Omega}_L) \\
&= \frac{1}{8\pi}\int_{4\pi} d\underline{\Omega}^* \; g_L(\underline{\Omega}_L)\,K(\kappa, \alpha')\,F_r(n, \alpha')\,\delta_2(\underline{\Omega} \bullet \underline{\Omega}^*) \\
&= \frac{1}{8\pi} g_L(\underline{\Omega}_L^*)\,K(\kappa, \alpha^*)\,F_r(n, \alpha^*) \qquad (28)
\end{aligned}$$

where $\Omega_L^* = \Omega_L^*(\underline{\Omega}', \underline{\Omega})$ defines leaf normals condusive for specular reflection given the incident and exit photon directions.

The scattering coefficient for specular reflection from the leaf surface σ_s' has the form,

$$\begin{aligned}
\sigma_s'(\underline{r}, \underline{\Omega}') &= u_L(\underline{r})\,\frac{1}{\pi}\int_{4\pi} d\underline{\Omega}\;\Gamma_s(\underline{\Omega}' \rightarrow \underline{\Omega}), \\
&= u_L(\underline{r})\,\frac{1}{2\pi}\int_{2\pi+} d\underline{\Omega}_L \; g_L(\underline{\Omega}_L)\,|\underline{\Omega}' \bullet \underline{\Omega}_L|\,K(\kappa(\alpha')\,F_r(n, \alpha'), \qquad (29) \\
&= u_L(\underline{r})\,\Gamma_s(\underline{\Omega}').
\end{aligned}$$

The normalized scattering phase function is therefore,

$$P_s(\underline{\Omega}' \to \underline{\Omega}) = \frac{4\Gamma_s(\underline{\Omega}' \to \underline{\Omega})}{G_s(\underline{\Omega}')}, \tag{30}$$

such that,

$$\frac{1}{4\pi} \int_{4\pi} d\underline{\Omega}\, P_s(\underline{\Omega}' \to \underline{\Omega}) = 1.$$

Problem Sets

- **Problem 1.** Let $f(\gamma)$, $-1 \le \gamma \le 1$, be a function of one variable; $\underline{\Omega} \equiv (\theta, \varphi)$ and $\underline{\Omega}_L \equiv (\theta_L, \varphi_L)$ are two unit vectors. Show that

$$\int_{2\pi^+} f(\underline{\Omega}_L \bullet \underline{\Omega})\, d\underline{\Omega} = 4\pi\, q(\sin\theta_L).$$

  Here $\underline{\Omega} \bullet \underline{\Omega}_L$ is the scalar product of two vectors, and q(x), $0 \le x \le 1$, is a function of one variable defined as

$$q(x) = \frac{1}{2}\int_x^1 f(\gamma)d\gamma + \frac{1}{2}\int_0^x [\alpha(\gamma, x)f(\gamma) + \beta(\gamma, x)f(-\gamma)]d\gamma,$$

  where $\alpha(\gamma, x) + \beta(\gamma, x) = 1$, and

$$\beta(\gamma, x) = \frac{1}{\pi}\arccos\frac{\gamma\sqrt{1-x^2}}{x\sqrt{1-\gamma^2}}.$$

- **Problem 2.** Letting $f(\gamma) = |\gamma|$, show that

$$\int_{2\pi^+} |\underline{\Omega}_L \bullet \underline{\Omega}|\, d\underline{\Omega} = \pi.$$

- **Problem 3.** Show that the leaf albedo for the bi-Lambertian model is

$$\int_{4\pi} d\underline{\Omega}\, \gamma_{L,d}(\underline{\Omega}' \to \underline{\Omega}, \underline{\Omega}_L) = \rho_{L,d} + \tau_{L,d}.$$

- **Problem 4.** Prove (14).

- **Problem 5.** Show that the geometry factor $G(\underline{r}, \underline{\Omega})$ for spherically distributed leaf normals depends neither $\underline{r}$ nor $\underline{\Omega}$ and is equal to 0.5.

- **Problem 6.** Show that $G = \mu$ for horizontal leaves, and $G = (2/\pi)\sin\theta$ for vertical leaves.

- **Problem 7.** Let the polar angle, θ_L, and azimuth, φ_L, of leaf normals are independent (see Eq. 3). Show that

$$G(\underline{r},\mu) = \int_0^1 d\mu_L \, \overline{g}_L(\underline{r},\mu_L)\,\psi(\mu,\mu_L),$$

where $\mu_L = \cos\theta_L$, $\mu = \cos\theta$, and

$$\psi(\mu,\mu_L) = \frac{1}{2\pi}\int_0^{2\pi} h(\varphi_L)\,|\underline{\Omega}\bullet\underline{\Omega}_L|\,d\varphi_L\ .$$

- **Problem 8.** Show that in canopies where leaf normals are distributed uniformly along the azimuthal coordinate [i.e., $h(\varphi_L) = 1$], $\psi(\mu,\mu_L)$ can be reduced to

$$\psi(\mu,\mu_L) = \begin{cases} |\mu\mu_L|, & \text{if } |\mu\mu_L| \geq |\sin\theta\sin\theta_L|, \\ \mu\mu_L(2\varphi_t/\pi - 1) + (2/\pi)\sqrt{1-\mu^2}\sqrt{1-\mu_L^2}\,\sin\varphi_t, & \text{otherwise,} \end{cases}$$

where the branch angle φ_t is $\arccos(-\cot\theta\times\cot\theta_L)$.

- **Problem 9.** Show that in canopies with constant leaf normal inclination but uniform orientation along the azimuth [cf. Eq. (4)], $G(\mu) = \psi(\mu,\mu_L)$.

- **Problem 10.** Using Eq. (6), derive the $\psi(\mu,\mu_L)$ in the case of heliotropic orientations.

- **Problem 11.** Given the direction of incoming, $\underline{\Omega}$, and reflected, $\underline{\Omega}'$, fluxes at the leaf surface ($\|\underline{\Omega}\| = \|\underline{\Omega}'\| = 1$) show that the direction of leaf normals $\underline{n}_L(\mu_L,\varphi_L)$ in the case of specular reflection is given by

$$\mu_L = \frac{|\mu' - \mu|}{\sqrt{2(1-\underline{\Omega}'\bullet\underline{\Omega})}}$$

$$\tan\varphi_L = \frac{\sqrt{1-\mu'^2}\,\sin\varphi' - \sqrt{1-\mu^2}\,\sin\varphi}{\sqrt{1-\mu'^2}\,\cos\varphi' - \sqrt{1-\mu^2}\,\cos\varphi}$$

References

Allen W.A., H.W. Gausman, A.J. Richardson, and J.R. Thomas (1969). Interaction of isotropic light with a compact leaf. *J. Opt. Soc. Amer.*. **59**, 1376-1379.

Bunnik, N.J.J. (1978). The multispectral reflectance of shortwave radiation by agricultural crops in relation with their morphological and optical properties. Pudoc Publications, Wageningen, The Netherlands.

Goel, N.S. and D.E. Strebel, (1984). Simple Beta distribution representation of leaf orientation in vegetation canopies. *Agron, J*., **76**, 800-802.

Jacquemoud S. and F. Baret F. (1990). PROSPECT: a model of leaf optical properties spectra. *Remote Sens. Environ.,* 34:75-91.

Knyazikhin, Y., J.Kranigk, G. Miessen, O. Panfyorov, N. Vygodskaya, and G. Gravenhorst (1996). Modeling three-dimensional distribution of photosynthetically active radiation in sloping coniferous stands, *Biomass and Bioenergy*. **11**, 2/3: 189-200.

Knyazikhin, Y., J.V., Martonchik, R.B. Myneni, D.J. Diner, and S.W. Running (1998). Synergistic algorithm for estimating vegetation canopy leaf area index and fraction of absorbed photosynthetically active radiation from MODIS and MISR data. *J. Geophys. Res*., **103,** 32257-32275.

Lang, A.R.G. (1991). Application of some of Cauchy's theorems to estimation of surface areas of leaves, needles and branches of plants, and light transmittance. *Agric. For. Meteorol*. **55**,191-212.

Oker-Blom, P. and S. Kellomäki (1982). Effect of angular distribution of foliage on light absorption and photosynthesis in the plant canopy: Theoretical computations. *Agric. For. Meteorol*. **26**, 105-116.

Oker-Blom, P. and H. Smolander (1988). The ratio of shoot silhouette area to total needle area in Scots pine. *Forest Science* **34**, 894-906.

Ross, J. (1981). *The Radiation Regime and Architecture of Plant Stands*. Dr. W. Junk Publishers, Delft, The Netherlands.

Shultis, K.S. and R.B. Myneni (1988). Radiative transfer in vegetation canopies with anisotropic scattering. *J. Quant. Spectroscp. Radiat. Trans*., **39**, 115-129.

Stenberg, P. (1996). Simulations of the effects of shoot structure and orientation on vertical gradients in intercepted light by conifer canopies. *Tree Physiology,* **16**, 99-108.

Vanderbilt, V.C., L. Grant, and S.L. Ustin (1991). Polarization of light by vegetation. In *Photon-Vegetation Interactions: Applications in Optical remote Sensing and Plant Ecology*, R.B. Myneni and J. Ross (eds.), Springer Verlag, Berlin Heildelberg, pp. 191-228.

Verstrate, M.M. (1987). Radiation transfer in plant canopies: transmission of direct solar radiation and the role of leaf orientation. *J. Geophys. Res*., **92,** 10985-10995.

Further Readings

Myneni, R.B., J. Ross, and G. Asrar (1989). A review on the theory of photon transport in leaf canopies. *Agric. For. Meteorol*., **45**, 1-153.

Ross, J. (1981). *The Radiation Regime and Architecture of Plant Stands*. Dr. W. Junk Publishers, Delft, The Netherlands.

Myneni, R.B. and J. Ross (eds.) (1991). *Photon-Vegetation Interactions: Applications in Optical remote Sensing and Plant Ecology*, Springer Verlag, Berlin Heildelberg.

Chapter 2 Derivations by Shabanov et al.

Problem 1. Let $f(\gamma)$, $-1 \le \gamma \le 1$, be a function of one variable, $\underline{\Omega} \equiv (\theta, \varphi)$ and $\underline{\Omega}_L \equiv (\theta_L, \varphi_L)$ are two unit vectors. Show that

$$\int_{2\pi^+} f(\underline{\Omega}_L \bullet \underline{\Omega})\, d\underline{\Omega} = 4\pi\, q(\sin\theta_L)\,.$$

Here $\underline{\Omega} \bullet \underline{\Omega}_L$ is the scalar product of two vectors, and q(x), $0 \le x \le 1$, is a function of one variable defined as

$$q(x) = \frac{1}{2}\int_x^1 f(\gamma)d\gamma + \frac{1}{2}\int_0^x [\alpha(\gamma, x)f(\gamma) + \beta(\gamma, x)f(-\gamma)]d\gamma\,,$$

where $\alpha(\gamma, x) + \beta(\gamma, x) = 1$, and

$$\beta(\gamma, x) = \frac{1}{\pi}\arccos\frac{\gamma\sqrt{1-x^2}}{x\sqrt{1-\gamma^2}}\,.$$

Solution. Let

$$g(\underline{\Omega}_L) \equiv \int_{2\pi^+} f(\underline{\Omega}_L \bullet \underline{\Omega})\, d\underline{\Omega}\,. \tag{1}$$

In the following derivations we assume that $\varphi_L = 0$, that is, vector $\underline{\Omega}_L$ belongs to ZX plane. This assumption does not limit the generality of the derivations as one always can substitute φ with $(\varphi - \varphi_L)$ without changing the domain of the integration (i.e., the upper hemisphere). For convenience of derivations let us transform the original system of coordinates to a new one, where $\underline{\Omega}_L$ is aligned with Z-direction (Fig. 1). This can be accomplished with rotation by angle $-\theta_L$ around the Y-axis as specified with the following linear transform,

$$\underline{R}' \equiv \hat{A}(-\theta_L)\,\underline{R},$$

where

$$\hat{A}(-\theta_L) \equiv \begin{bmatrix} \cos\theta_L & 0 & -\sin\theta_L \\ 0 & 1 & 0 \\ \sin\theta_L & 0 & \cos\theta_L \end{bmatrix}$$

and $\underline{R} = (x, y, z)$ and $\underline{R}' = (x', y', z')$ are vectors in the original and new coordinate system, respectively. Note the minus sign for angle θ_L. This is due to the fact that positive angles are counted *outward from* Z-direction. One example of transformation is for the Z-axis, which is

transformed from $\underline{Z} = (0,0,1)$ in the original system into $\underline{Z'} = (-\sin\theta_L,\ 0,\ \cos\theta_L)$ in the new system.

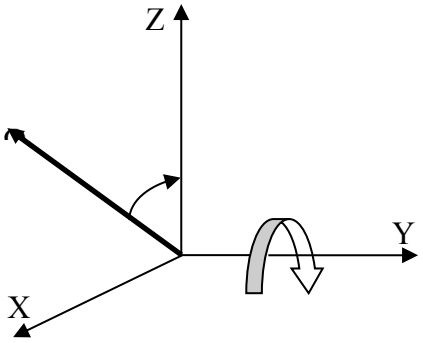

Figure. 1 Coordinate system transform via rotation by angle $-\theta_L$ around the Y-axis.

To determine the integration domain in the new coordinate system, let $\underline{v} = (\sin\theta\cos\varphi,\ \sin\theta\sin\varphi,\ \cos\theta)$ be a unit vector in the new system. The $\underline{v}$ vector falls into the upper hemisphere of the original system if and only if

$$\underline{v} \bullet \underline{z'} \equiv -\sin\theta_L \cdot \sin\theta\cos\varphi + 0 \cdot \sin\theta\sin\varphi + \cos\theta_L \cdot \cos\theta \geq 0.$$

Therefore,

$$\cos\varphi \leq \frac{\cos\theta_L \cos\theta}{\sin\theta_L \sin\theta}. \tag{2}$$

Note that the angular domain of the upper hemisphere in the original coordinate system is $\theta \in [0,\pi]$ and $\varphi \in [0,2\pi]$. This domain is specified differently in the new coordinate system as shown in Fig. 2. Namely, three sectors with respect to θ can be identified: $\theta \in [0, \pi/2 - \theta_L]$ (shown in Red), $\theta \in [\pi/2 - \theta_L, \pi/2 + \theta_L]$ (shown in green), and $\theta \in [\pi/2 + \theta_L, \pi]$ (shown in blue). The corresponding variations of φ can be derived from the algebraic analysis of Eq. (2). The final expression for the angular domain in the new coordinate system is:

$$\begin{cases} \dfrac{\cos\theta_L \cos\theta}{\sin\theta_L \sin\theta} > 1, & \theta \in [0, \dfrac{\pi}{2} - \theta_L), \\ & \varphi \in [0,\ 2\pi]; \\ -1 \leq \dfrac{\cos\theta_L \cos\theta}{\sin\theta_L \sin\theta} \leq 1, & \theta \in [\dfrac{\pi}{2} - \theta_L, \dfrac{\pi}{2} + \theta_L], \\ & \varphi \in [\arccos\dfrac{\cos\theta_L \cos\theta}{\sin\theta_L \sin\theta},\ 2\pi - \arccos\dfrac{\cos\theta_L \cos\theta}{\sin\theta_L \sin\theta}]; \\ \dfrac{\cos\theta_L \cos\theta}{\sin\theta_L \sin\theta} < -1, & \theta \in (\dfrac{\pi}{2} + \theta_L, \pi], \\ & \varphi \in \varnothing. \end{cases} \tag{3}$$

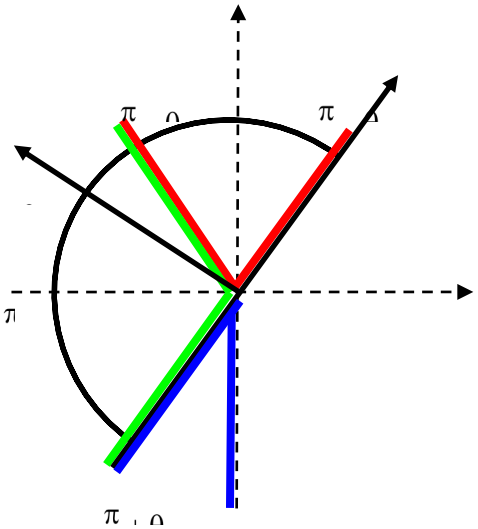

Figure. 2 The upper hemisphere of the original system of coordinates XYZ in a new system of coordinates $X'Y'Z'$. Vector $\underline{\Omega}_L$ is aligned with axis Z' of the new system.

In a view that in the new coordinate system the direction $\underline{\Omega}_L$ coincides with Z', the argument of function $f(\underline{\Omega}_L \bullet \underline{\Omega})$ in Eq. (1) simplifies, i.e., $\underline{\Omega}_L \bullet \underline{\Omega} = \cos\theta$. Therefore,

$$g(\underline{\Omega}_L) \equiv \int_{2\pi^+} f(\underline{\Omega}_L \bullet \underline{\Omega})\, d\underline{\Omega} = \int_{\cos\varphi \le \frac{\cos\theta_L \cos\theta}{\sin\theta_L \sin\theta}} f(\cos\theta)\, d\underline{\Omega}$$

$$= \int_0^{\frac{\pi}{2}-\theta_L} f(\cos\theta)(-d\cos\theta) \int_0^{2\pi} d\varphi + \int_{\frac{\pi}{2}-\theta_L}^{\frac{\pi}{2}+\theta_L} f(\cos\theta)(-d\cos\theta) \int_{\arccos\left(\frac{\cos\theta_L \cos\theta}{\sin\theta_L \sin\theta}\right)}^{2\pi-\arccos\left(\frac{\cos\theta_L \cos\theta}{\sin\theta_L \sin\theta}\right)} d\varphi$$

$$= 2\pi \int_{\theta_L}^{\frac{\pi}{2}} f(\sin\theta)\, d(\sin\theta)$$

$$+ \int_0^{\theta_L} f(\sin\theta) \left[2\pi - 2\arccos\left(\frac{\cos\theta_L \cos\theta}{\sin\theta_L \sin\theta} \right) \right] d(\sin\theta)$$

$$+ \int_0^{\theta_L} f(-\sin\theta) \left[2\arccos\left(\frac{\cos\theta_L \cos\theta}{\sin\theta_L \sin\theta} \right) \right] d(\sin\theta). \qquad (4)$$

Note that in the last step of derivations we substituted θ with $\pi/2 - \theta$, and accounted for the fact that $\cos\theta = \sin(\pi/2 - \theta)$, $\sin\theta = \cos(\pi/2 - \theta)$, and $\arccos(-\psi) = \pi - \arccos(\psi)$. Finally, let $x = \sin(\theta_L)$, $\gamma = \sin(\theta)$, and

$$\beta(\gamma, x) = \frac{1}{\pi} \arccos\left(\frac{\cos\theta_L \sin\theta}{\sin\theta_L \cos\theta} \right) = \frac{1}{\pi} \arccos \frac{\gamma\sqrt{1-x^2}}{x\sqrt{1-\gamma^2}},$$

$$\alpha(\gamma, x) = 1 - \beta(\gamma, x).$$

Substituting the new variables in Eq. (4) and changing the limits of integration according to the variable γ, we finally have

$$g(\underline{\Omega}_L) = 2\pi\int_x^1 f(\gamma)d\gamma + 2\pi\int_0^x [\alpha(\gamma, x)f(\gamma) + \beta(\gamma, x)f(-\gamma)]d\gamma = 4\pi q(x).$$

Problem 2. Letting $f(\gamma) = |\gamma|$, show that

$$\int_{2\pi^+} |\underline{\Omega}_L \bullet \underline{\Omega}| d\underline{\Omega} = \pi.$$

Solution. According to the results of Problem 1

$$\int_{2\pi^+} |\underline{\Omega}_L \bullet \underline{\Omega}| d\underline{\Omega} \equiv \int_{2\pi^+} f(|\gamma|) d\underline{\Omega} = 4\pi \frac{1}{2}\left[\int_x^1 \gamma d\gamma + \int_0^z [\alpha(\gamma, x) + \beta(\gamma, x)]\gamma d\gamma\right].$$

Taking into account that $\alpha(\lambda, x) + \beta(\lambda, x) = 1$ (cf. Problem 1), we have

$$\int_{2\pi^+} |\underline{\Omega}_L \bullet \underline{\Omega}| d\underline{\Omega} = 2\pi\left[\int_x^1 \gamma\, d\gamma + \int_0^z \gamma\, d\gamma\right] = 2\pi\int_0^1 \gamma\, d\gamma = \pi.$$

Problem 3. Show that the leaf albedo for the bi-Lambertian model is

$$\int_{4\pi} d\underline{\Omega}\, \gamma_{L,d}(\underline{\Omega}' \to \underline{\Omega}, \underline{\Omega}_L) = \rho_{L,d} + \tau_{L,d}.$$

Solution. The bi-Lambertian model for diffuse leaf scattering phase function is,

$$\gamma_{L,d}(\underline{\Omega}' \to \underline{\Omega}, \underline{\Omega}_L) = \begin{cases} \frac{1}{\pi}\rho_{L,d}|\underline{\Omega} \bullet \underline{\Omega}_L|, & (\underline{\Omega} \bullet \underline{\Omega}_L)(\Omega' \bullet \underline{\Omega}_L) < 0, \\ \frac{1}{\pi}\tau_{L,d}|\underline{\Omega} \bullet \underline{\Omega}_L|, & (\underline{\Omega} \bullet \underline{\Omega}_L)(\underline{\Omega}' \bullet \underline{\Omega}_L) > 0. \end{cases} \quad (1)$$

Note that the angles $\underline{\Omega}'$ and $\underline{\Omega}_L$ are fixed in the integral of interests and integration over whole sphere can be spitted into two parts, namely,

$$\int_{4\pi} d\underline{\Omega}\, \gamma_{L,d}(\underline{\Omega}' \to \underline{\Omega}, \underline{\Omega}_L)$$

$$= \int\limits_{(\underline{\Omega}\bullet\underline{\Omega}_L)(\underline{\Omega}'\bullet\underline{\Omega}_L)>0} d\underline{\Omega} \quad \gamma_{L,d}(\underline{\Omega}' \to \underline{\Omega}, \underline{\Omega}_L) + \int\limits_{(\underline{\Omega}\bullet\underline{\Omega}_L)(\underline{\Omega}'\bullet\underline{\Omega}_L)<0} d\underline{\Omega} \quad \gamma_{L,d}(\underline{\Omega}' \to \underline{\Omega}, \underline{\Omega}_L). \tag{2}$$

Taking into account Eq. (1), we have

$$\int\limits_{(\underline{\Omega}\bullet\underline{\Omega}_L)(\underline{\Omega}'\bullet\underline{\Omega}_L)>0} d\underline{\Omega} \quad \gamma_{L,d}(\underline{\Omega}' \to \underline{\Omega}, \underline{\Omega}_L) = \frac{1}{\pi}\tau_{L,d} \int\limits_{(\underline{\Omega}\bullet\underline{\Omega}_L)(\underline{\Omega}'\bullet\underline{\Omega}_L)>0} d\underline{\Omega} \quad \left|\underline{\Omega}\bullet\underline{\Omega}_L\right|, \tag{3a}$$

$$\int\limits_{(\underline{\Omega}\bullet\underline{\Omega}_L)(\underline{\Omega}'\bullet\underline{\Omega}_L)<0} d\underline{\Omega} \quad \gamma_{L,d}(\underline{\Omega}' \to \underline{\Omega}, \underline{\Omega}_L) = \frac{1}{\pi}\rho_{L,d} \int\limits_{(\underline{\Omega}\bullet\underline{\Omega}_L)(\underline{\Omega}'\bullet\underline{\Omega}_L)<0} d\underline{\Omega} \quad \left|\underline{\Omega}\bullet\underline{\Omega}_L\right|. \tag{3b}$$

In view that the angles $\underline{\Omega}'$ and $\underline{\Omega}_L$ are fixed, the integrals on the right hand side of Eqs. (3a) and (3b) are identical and equal to the integral over hemisphere ($2\pi^+$ or $2\pi^-$). The last integral was evaluated in the Problem 2, namely,

$$\int\limits_{2\pi^+} d\underline{\Omega} \left|\underline{\Omega}\bullet\underline{\Omega}_L\right| = \pi. \tag{4}$$

Combining Eqs. (2)-(4) we finally have

$$\int\limits_{4\pi} d\underline{\Omega}\, \gamma_{L,d}(\underline{\Omega}' \to \underline{\Omega}, \underline{\Omega}_L) = \frac{1}{\pi}\tau_{L,d}\pi + \frac{1}{\pi}\rho_{L,d}\pi = \tau_{L,d} + \rho_{L,d}.$$

Problem 5. Prove

$$\frac{1}{2\pi}\int\limits_{2\pi^+} d\underline{\Omega}\, G(\underline{r}, \underline{\Omega}) = \frac{1}{2}, \tag{1}$$

Solution. Note,

$$G(\underline{r}, \underline{\Omega}) = \frac{1}{2\pi}\int\limits_{2\pi^+} d\underline{\Omega}_L \; g_L(\underline{\Omega}_L)\left|\underline{\Omega}_L \bullet \underline{\Omega}\right|, \tag{2a}$$

$$\frac{1}{2\pi}\int\limits_{2\pi+} d\underline{\Omega}_L \; g_L(\underline{\Omega}_L) = 1. \tag{2b}$$

Combining Eq. (1)-(2) and result of Problem 2, we have

$$\frac{1}{2\pi}\int\limits_{2\pi^+} d\underline{\Omega}\, G(\underline{r}, \underline{\Omega})$$

$$= \frac{1}{2\pi} \int_{2\pi^+} d\underline{\Omega} \, \frac{1}{2\pi} \int_{2\pi^+} d\underline{\Omega}_L \; g_L(\underline{\Omega}_L) \left| \underline{\Omega}_L \bullet \underline{\Omega} \right|$$

$$= \frac{1}{4\pi^2} \int_{2\pi^+} d\underline{\Omega}_L \; g_L(\underline{\Omega}_L) \int_{2\pi^+} d\underline{\Omega} \left| \underline{\Omega}_L \bullet \underline{\Omega} \right|$$

$$= \frac{1}{4\pi^2} 2\pi \cdot \pi = \frac{1}{2}.$$

Problem 6. Show that the geometry factor $G(\underline{r}, \underline{\Omega})$ for spherically distributed leaf normals depends neither $\underline{r}$ nor $\underline{\Omega}$ and is equal to 0.5.

Solution. Recall,

$$G(\underline{r}, \underline{\Omega}) = \frac{1}{2\pi} \int_{2\pi^+} d\underline{\Omega}_L \; g_L(\underline{\Omega}_L) \left| \underline{\Omega}_L \bullet \underline{\Omega} \right|.$$

Recall also, that for spherically distributed leaf normals $g_L(\underline{\Omega}_L) = 1$. Combining this result with the result of the Problem 2, we have

$$G(\underline{r}, \underline{\Omega}) = \frac{1}{2\pi} \int_{2\pi^+} d\underline{\Omega}_L \left| \underline{\Omega}_L \bullet \underline{\Omega} \right| = \frac{1}{2\pi} \cdot \pi = \frac{1}{2}.$$

Problem 7. Show that $G = \mu$ for horizontal leaves, and $G = (2/\pi)\sin\theta$ for vertical leaves.

Solution. Recall,

$$G(\underline{r}, \underline{\Omega}) = \frac{1}{2\pi} \int_{2\pi^+} d\underline{\Omega}_L \; g_L(\underline{\Omega}_L) \left| \underline{\Omega}_L \bullet \underline{\Omega} \right|.$$

Further, let $\underline{\Omega} = (\sin\theta\cos\varphi, \sin\theta\sin\varphi, \cos\theta)$ and $\underline{\Omega}_L = (\sin\theta_L \cos\varphi_L, \sin\theta_L \sin\varphi_L, \cos\theta_L)$. Therefore,

$$\begin{aligned} \underline{\Omega}_L \bullet \underline{\Omega} &= (\sin\theta_L \cos\varphi_L) \cdot (\sin\theta\cos\varphi) + (\sin\theta_L \sin\varphi_L) \cdot (\sin\theta\sin\varphi) + (\cos\theta_L) \cdot (\cos\theta) \\ &= \sin\theta_L \sin\theta \cdot \cos(\varphi_L - \varphi) + \cos\theta_L \cos\theta. \end{aligned}$$

For *horizontal leaves* the derivations for $G(\underline{r}, \underline{\Omega})$ are as follows. The probability density of leaf normal orientation is

$$g_L(\underline{\Omega}_L) = \frac{\delta(\theta_L - 0)}{\sin\theta_L}.$$

Therefore,

$$G(\underline{r},\underline{\Omega}) = \frac{1}{2\pi}\int_0^{\pi/2} \sin\theta_L d\theta_L \int_0^{2\pi} d\varphi_L\, g_L(\underline{\Omega}_L)\left|\underline{\Omega}_L \bullet \underline{\Omega}\right|$$

$$= \frac{1}{2\pi}\int_0^{\pi/2} d\theta_L \int_0^{2\pi} d\varphi_L \sin\theta_L \frac{\delta(\theta_L - 0)}{\sin\theta_L}\left|\sin\theta_L \sin\theta\cdot\cos(\varphi_L - \varphi) + \cos\theta_L \cos\theta\right|$$

$$= \left|\cos\theta\right| \equiv \mu.$$

Similar derivations can be performed for *vertical leaves*. In this case the probability density of leaf normal orientation is

$$g_L(\underline{\Omega}_L) = \frac{\delta(\theta_L - \pi/2)}{\sin\theta_L}.$$

Therefore,

$$G(\underline{r},\underline{\Omega}) = \frac{1}{2\pi}\int_0^{\pi/2} d\theta_L \int_0^{2\pi} d\varphi_L \sin\theta_L \frac{\delta(\theta_L - \pi/2)}{\sin\theta_L}\left|\sin\theta_L \sin\theta\cdot\cos(\varphi_L - \varphi) + \cos\theta_L \cos\theta\right|$$

$$= \frac{1}{2\pi}\int_0^{2\pi} d\varphi_L \left|1\cdot\sin\theta\cdot\cos(\varphi_L - \varphi) + 0\right| = \frac{2}{\pi}\left|\sin\theta\right|.$$

Problem 8. Let the polar angle, θ_L, and azimuth, φ_L, of leaf normals be independent. Show that

$$G(\underline{r},\mu) = \int_0^1 d\mu_L \bar{g}_L(\underline{r},\mu_L)\psi(\mu,\mu_L),$$

where $\mu_L = \cos\theta_L$, $\mu = \cos\theta$, and

$$\psi(\mu,\mu_L) = \frac{1}{2\pi}\int_0^{2\pi} h_L(\varphi_L)\,|\,\underline{\Omega}\bullet\underline{\Omega}_L\,|\,d\varphi_L\ .$$

Solution. Since the polar angle, θ_L, and azimuth angle, φ_L, of leaf normals are independant, the following representation of the probability density of leaf normal orientation is valid:

$$g_L(\underline{\Omega}_L) = \bar{g}_L(\mu_L)\, h_L(\varphi_L),$$

where $\bar{g}_L(\mu_L)$ and $h_L(\varphi_L)/2\pi$ are the probability density functions of leaf normal inclination and azimuth, respectively. Therefore,

$$\begin{aligned} G(\underline{r},\mu_L) &= \frac{1}{2\pi}\int_{2\pi^+} d\underline{\Omega}_L\; g_L(\underline{r},\underline{\Omega}_L)\left|\underline{\Omega}_L \bullet \underline{\Omega}\right| \\ &= \frac{1}{2\pi}\int_0^1 d\mu_L \int_0^{2\pi} d\varphi_L\, \bar{g}_L(\underline{r},\mu_L)\, h_L(\varphi_L)\left|\underline{\Omega}_L \bullet \underline{\Omega}\right| \\ &= \frac{1}{2\pi}\int_0^1 d\mu_L\, \bar{g}_L(\underline{r},\mu_L)\int_0^{2\pi} d\varphi_L\; h_L(\varphi_L)\left|\underline{\Omega}_L \bullet \underline{\Omega}\right| \\ &= \frac{1}{2\pi}\int_0^1 d\mu_L\, \bar{g}_L(\underline{r},\mu_L)\,\psi(\mu,\mu_L). \end{aligned}$$

Problem 9. Show that in canopies where leaf normals are distributed uniformly along the azimuthal coordinate [i.e., $h_L(\varphi_L) = 1$], $\psi(\mu,\mu_L)$ can be reduced to

$$\psi(\mu,\mu_L) = \begin{cases} |\mu\,\mu_L|, & \text{if } |\mu\,\mu_L| \ge |\sin\theta \sin\theta_L|, \\ \mu\mu_L(2\varphi_t/\pi - 1) + (2/\pi)\sqrt{1-\mu^2}\,\sqrt{1-\mu_L^2}\,\sin\varphi_t, & \text{otherwise,} \end{cases}$$

where the branch angle φ_t is $\arccos(-\cot\theta \times \cot\theta_L)$.

Solution. Recall (cf. Problem 6),

$$\underline{\Omega}_L \bullet \underline{\Omega} = \sin\theta_L \sin\theta \cdot \cos(\varphi_L - \varphi) + \cos\theta_L \cos\theta.$$

Therefore,

$$\begin{aligned} \psi(\mu,\mu_L) &\equiv \frac{1}{2\pi}\int_0^{2\pi} d\varphi_L\, h_L(\varphi_L)\left|\underline{\Omega}_L \bullet \underline{\Omega}\right| \\ &= \frac{1}{2\pi}\int_0^{2\pi} d\varphi_L \left|\sin\theta_L \sin\theta\cos(\varphi_L - \varphi) + \cos\theta_L \cos\theta\right| \\ &= \frac{1}{\pi}\int_0^{\pi} d\varphi_L \left|\sin\theta_L \sin\theta\cos(\varphi_L - \varphi) + \cos\theta_L \cos\theta\right| \end{aligned}$$

$$= \frac{1}{\pi}\int_0^{\pi} d\varphi_L \left| \sin\theta_L \sin\theta \cdot \left(\cos\varphi_L + \mathrm{ctg}\,\theta_L \mathrm{ctg}\,\theta\right)\right| \tag{1}$$

Note that in the above derivations we took into account that $h_L(\varphi_L) = 1$ and also symmetry of function $(a \cdot \cos(\xi) + b)$ in the interval $\xi \in [0, 2\pi]$. In the derivations to follow we need to consider two cases. First, consider the case, when $\left|\mathrm{ctg}\theta_L \mathrm{ctg}\theta\right| \geq 1$. In this case the expression $(\cos\varphi_L + \mathrm{ctg}\,\theta_L \mathrm{ctg}\,\theta)$ in the Eq. (1) does not change the sign over the whole interval of integration, $[0, \pi]$. Therefore,

$$\begin{aligned}
\psi(\mu, \mu_L) &\equiv \frac{1}{\pi}\int_0^{\pi} d\varphi_L \left| \sin\theta_L \sin\theta \cdot \left(\cos\varphi_L + \mathrm{ctg}\,\theta_L \mathrm{ctg}\,\theta\right)\right| \\
&= \frac{1}{\pi}\left|\int_0^{\pi} d\varphi_L \sin\theta_L \sin\theta \cdot \left(\cos\varphi_L + \mathrm{ctg}\theta_L \mathrm{ctg}\theta\right)\right| \\
&= \left|\cos\theta_L \cos\theta\right|. \qquad (2a)
\end{aligned}$$

Now consider the second case, when $\left|\mathrm{ctg}\theta_L \mathrm{ctg}\theta\right| < 1$. Here the value of the expression $(\cos\varphi_L + \mathrm{ctg}\,\theta_L \mathrm{ctg}\,\theta)$ in the Eq. (1) is monotonically decreasing in the interval $\varphi \in [0, \pi]$. The value of $\varphi = \varphi^*$, where the integrand changes the sign is given by

$$\cos\varphi^* + \mathrm{ctg}\,\theta_L \mathrm{ctg}\,\theta = 0 \;\Rightarrow \varphi^* = \arccos\left[-\mathrm{ctg}\,\theta_L \mathrm{ctg}\,\theta\right].$$

Now we can evaluate Eq. (1) by splitting the interval of integration into two parts, where the integrand has the opposite signs,

$$\begin{aligned}
\psi(\mu, \mu_L) &\equiv \frac{1}{\pi}\int_0^{\pi} d\varphi_L \left| \sin\theta_L \sin\theta \cdot \left(\cos\varphi_L + \mathrm{ctg}\,\theta_L \mathrm{ctg}\,\theta\right)\right| \\
&= \frac{1}{\pi}\left|\int_0^{\varphi^*} d\varphi_L \left(\sin\theta_L \sin\theta \cos\varphi_L + \cos\theta_L \cos\theta\right) - \int_{\varphi^*}^{\pi} d\varphi_L \left(\sin\theta_L \sin\theta \cos\varphi_L + \cos\theta_L \mathrm{ctg}\,\theta\right)\right| \\
&= \frac{1}{\pi}\left| 2\sin\theta_L \sin\theta \sin\varphi^* + \cos\theta_L \cos\theta\left(2\varphi^* - \pi\right)\right|. \qquad (2b)
\end{aligned}$$

Combined, the Eq. (2a)-(2b) present the solution to the problem.

Problem 10. Show that in canopies with constant leaf normal inclination but uniform orientation along the azimuth, $G(\mu) = \psi(\mu, \mu_L)$

Solution. For canopies with independent polar angle, θ_L, and azimuth, φ_L, of leaf normals (cf. Problem 7), we have

$$G(\underline{r},\mu) = \int_0^1 d\mu_L \bar{g}_L(\underline{r},\mu_L)\psi(\mu,\mu_L), \tag{1}$$

where $\mu_L = \cos\theta_L$, $\mu = \cos\theta$, and

$$\psi(\mu,\mu_L) = \frac{1}{2\pi}\int_0^{2\pi} h_L(\varphi_L)\,|\,\underline{\Omega}\bullet\underline{\Omega}_L\,|\,d\varphi_L\,. \tag{2}$$

The condition of constant leaf normal inclination and uniform orientation along azimuth implies

$$\bar{g}_L(\underline{r},\mu_L) = \frac{\delta(\theta_L-\theta^*)}{\sin\theta_L} = \delta(\mu_L-\mu^*),$$
$$h_L(\varphi_L) = 1. \tag{3}$$

Combining Eqs. (1)-(3), we have

$$\begin{aligned} G(\underline{r},\mu) &= \int_0^1 d\mu_L \bar{g}_L(\underline{r},\mu_L)\psi(\mu,\mu_L) \\ &= \int_0^1 d\mu_L \delta(\mu_L-\mu^*)\psi(\mu,\mu_L), \\ &= \psi(\mu,\mu^*). \end{aligned}$$

Problem 11. Using Eq. (6), derive the $\psi(\mu,\mu_L)$ in the case of heliotropic orientations.

Solution. Recall (cf. Problem 7),

$$\psi(\mu,\mu_L) \equiv \frac{1}{2\pi}\int_0^{2\pi} h_L(\varphi_L)\,|\,\underline{\Omega}\bullet\underline{\Omega}_L\,|\,d\varphi_L. \tag{1}$$

In the case when the leaf azimuths have a preferred orientation with respect to the solar azimuth orientation (heliotropism) the h_L function may be modeled as follows,

$$\frac{1}{2\pi}h_L(\varphi_L,\varphi) = \frac{1}{\pi}\cos^2(\varphi-\varphi_L-\eta). \tag{2}$$

Recall also (cf. Problem 6),

$$\underline{\Omega}_L \bullet \underline{\Omega} = \sin\theta_L \sin\theta \cdot \cos(\varphi_L - \varphi) + \cos\theta_L \cos\theta. \tag{3}$$

Combining Eq. (1)-(3), we have

$$\begin{aligned}
\psi(\mu,\mu_L) &\equiv \frac{1}{2\pi}\int_0^{2\pi} h_L(\varphi_L)\,|\,\underline{\Omega}\bullet\underline{\Omega}_L\,|\,d\varphi_L \\
&= \frac{1}{\pi}\int_0^{2\pi} d\varphi_L \cos^2(\varphi - \varphi_L - \eta)\,|\sin\theta_L\sin\theta\cos(\varphi-\varphi_L)+\cos\theta_L\cos\theta\,| \\
&= \frac{1}{\pi}\int_0^{2\pi} d\alpha \cos^2(\alpha-\eta)\,|\sin\theta_L\sin\theta\cos\alpha+\cos\theta_L\cos\theta\,| \\
&= \frac{1}{\pi}\int_0^{2\pi} d\alpha \cos^2(\alpha-\eta)\,|\sin\theta_L\sin\theta\cdot(\cos\alpha+\mathrm{ctg}\,\theta_L\mathrm{ctg}\,\theta)\,|,
\end{aligned} \tag{4}$$

where $\alpha = \varphi - \varphi_L$. To evalute the above integral we need to consider two cases (cf. Problem 8). First, consider the case, when $|\mathrm{ctg}\theta_L\,\mathrm{ctg}\theta| \geq 1$. In this case the integrand does not change the sign over whole interval of integration. Therefore,

$$\begin{aligned}
\psi(\mu,\mu_L) &\equiv \frac{1}{\pi}\int_0^{2\pi} d\alpha \cos^2(\alpha-\eta)\,|\sin\theta_L\sin\theta\cos\alpha+\cos\theta_L\cos\theta)\,| \\
&= \frac{1}{\pi}\left|\int_0^{2\pi} d\alpha \cos^2(\alpha-\eta)\left[\sin\theta_L\sin\theta\cos\alpha+\cos\theta_L\cos\theta\right]\right| \\
&= \frac{1}{\pi}\left|\sin\theta_L\sin\theta\int_0^{2\pi} d\alpha\cos^2(\alpha-\eta)\cos\alpha + \cos\theta_L\cos\theta\int_0^{2\pi} d\alpha\cos^2(\alpha-\eta)\right|.
\end{aligned} \tag{5}$$

The evaluation of two definite integrals in Eq. (5) requires derivations of corresponding indefinite integrals, I_1 and I_2:

$$\begin{aligned}
I_1 &\equiv \sin\theta_L\sin\theta\int d\alpha\cos^2(\alpha-\eta)\cos\alpha = \sin\theta_L\sin\theta\int d\alpha\frac{1+\cos(2\alpha-2\eta)}{2}\cos\alpha \\
&= \frac{\sin\theta_L\sin\theta}{2}\left[\sin\alpha+\frac{\sin(\alpha-2\eta)}{2}+\frac{\sin(3\alpha-2\eta)}{6}\right].
\end{aligned} \tag{6a}$$

$$\begin{aligned}
I_2 &\equiv \cos\theta_L\cos\theta\int d\alpha\cos^2(\alpha-\eta) = \cos\theta_L\cos\theta\int d\alpha\frac{1+\cos(2\alpha-2\eta)}{2} \\
&= \frac{\cos\theta_L\cos\theta}{2}\left[\alpha+\frac{\sin(2\alpha-2\eta)}{2}\right].
\end{aligned} \tag{6b}$$

Therefore, the corresponding definite integrals over interval $\alpha \in [0,2\pi]$ are

$$I_1\big|_{\alpha=0}^{\alpha=2\pi} = 0 \text{ and } I_2\big|_{\alpha=0}^{\alpha=2\pi} = \pi \cos\theta_L \cos\theta. \tag{7}$$

Combining Eqs. (5)-(7), we have

$$\psi(\mu,\mu_L) = \left|\cos\theta\cos\theta_L\right| \equiv \mu\,\mu_L\,. \tag{8}$$

Now consider the second case, when $\left|\mathrm{ctg}\theta_L \mathrm{ctg}\theta\right| < 1$. In this case the expression under sign of integral in Eq. (4), $(\cos\alpha + \mathrm{ctg}\,\theta_L \mathrm{ctg}\,\theta)$, will change sign two times (first at α^* and second at $2\pi - \alpha^*$) over the interval $\alpha \in [0,2\pi]$. The value of α^* is given by

$$(\cos\alpha + \mathrm{ctg}\,\theta_L \mathrm{ctg}\,\theta) = 0 \;\Rightarrow \alpha^* = \arccos\left[-\mathrm{ctg}\,\theta_L \mathrm{ctg}\,\theta\right]. \tag{9}$$

In order to evaluate integral in Eq. (4) we need to consider three intervals, where integrand has constant sign: $\alpha \in [0,\alpha^*]$, $\alpha \in [\alpha^*, 2\pi - \alpha^*]$, and $\alpha \in [2\pi - \alpha^*, 2\pi]$. Therefore,

$$\begin{aligned}
\psi(\mu,\mu_L) &= \frac{1}{\pi}\int_0^{2\pi} d\alpha \left| \sin\theta_L \sin\theta \cos^2(\alpha - \eta)\cos\alpha + \cos\theta_L \cos\theta \cos^2(\alpha - \eta)\right| \\
&= \frac{1}{\pi}\left| \left[I_1 + I_2\right]\big|_0^{\alpha^*} - \left[I_1 + I_2\right]\big|_{\alpha^*}^{2\pi-\alpha^*} + \left[I_1 + I_2\right]\big|_{2\pi-\alpha^*}^{2\pi} \right| \\
&= \frac{1}{\pi}\left| \left[I_1 + I_2\right]\big|_0^{2\pi} - 2\cdot\left[I_1 + I_2\right]\Big|_{\alpha^*}^{2\pi-\alpha^*} \right| \qquad (10) \\
&= \frac{1}{\pi}\left| I_1\big|_0^{2\pi} - 2\cdot I_1\Big|_{\alpha^*}^{2\pi-\alpha^*} + I_2\big|_0^{2\pi} - 2\cdot I_2\Big|_{\alpha^*}^{2\pi-\alpha^*} \right|, \qquad (10)
\end{aligned}$$

where

$$I_1\big|_0^{2\pi} - 2\cdot I_1\Big|_{\alpha^*}^{2\pi-\alpha^*} = \sin\theta\sin\theta_L \cdot \left(2\sin\alpha^* + \sin\alpha^*\cos(2\eta) + \frac{1}{3}\sin(3\alpha^*)\cos(2\eta)\right), \tag{11a}$$

$$I_2\big|_0^{2\pi} - 2\cdot I_2\Big|_{\alpha^*}^{2\pi-\alpha^*} = \cos\theta\cos\theta_L \cdot \left(2\alpha^* - \pi + \sin(2\alpha^*)\cos(2\eta)\right). \tag{11b}$$

Combining Eqs. (10)-(11), we have

$$\begin{aligned}
\psi(\mu,\mu_L) = \Bigg| &\frac{\sin\theta\sin\theta_L}{\pi}\cdot\left(2\sin\alpha^* + \sin\alpha^*\cos(2\eta) + \frac{1}{3}\sin(3\alpha^*)\cos(2\eta)\right) \\
&+ \frac{\cos\theta\cos\theta_L}{\pi}\cdot\left(2\alpha^* - \pi + \sin(2\alpha^*)\cos(2\eta)\right)\Bigg|, \qquad (12)
\end{aligned}$$

where α^* is given by Eq. (9). Overall, Eqs. (8) and (12) present the complete solution to the problem. Finally, note that in the special case of dia-heliotropic distribution, ($\eta = 0$), the Eq. (12) reduces to

$$\psi(\mu,\mu_L) = \left| \frac{\sin\theta\sin\theta_L}{\pi} \cdot \left(3\sin\alpha^* + \frac{1}{3}\sin(3\alpha^*) \right) + \frac{\cos\theta\cos\theta_L}{\pi} \cdot \left(2\alpha^* - \pi + \sin(2\alpha^*) \right) \right|,$$

and in the case of para-heliotropic distribution ($\eta = \pi/2$), to

$$\psi(\mu,\mu_L) = \left| \frac{\sin\theta\sin\theta_L}{\pi} \cdot \left(2\sin\alpha^* - \frac{1}{3}\sin(3\alpha^*) \right) + \frac{\cos\theta\cos\theta_L}{\pi} \cdot \left(2\alpha^* - \pi - \sin(2\alpha^*) \right) \right|.$$

Problem 12. Calculate area scattering phase function for diffuse radiation, $\Gamma_d(\underline{\Omega}' \to \underline{\Omega})$, in the case of uniform leaf normal distribution, $g_L = 1$.

Solution. Recall,

$$\Gamma_d(\underline{\Omega}' \to \underline{\Omega}) = \rho_{L,d}\Gamma_d^-(\underline{\Omega}' \to \underline{\Omega}) + \tau_{L,d}\Gamma_d^+(\underline{\Omega}' \to \underline{\Omega}), \tag{1a}$$

where,

$$\Gamma_d^{\pm}(\underline{\Omega}' \to \underline{\Omega}) = \pm\frac{1}{2\pi}\int_0^1 d\mu_L \int_0^{2\pi} d\varphi_L \; g_L(\mu_L,\varphi_L)\,(\underline{\Omega}\bullet\underline{\Omega}_L)\,(\underline{\Omega}'\bullet\underline{\Omega}_L). \tag{1b}$$

The ($\pm$) in the above definition indicates that the φ_L integration is over that portion of the interval $[0,2\pi]$ for which the integrand is either positive (+) or negative (–). We need to calculate phase function for the case of uniform leaf normal orientation, $g_L = 1$. In view of the symmetry of the integrand with respect to $\underline{\Omega}_L$, the integral over the upper hemisphere is equal to that over lower hemisphere and,

$$\Gamma_d^{\pm}(\underline{\Omega}' \to \underline{\Omega}) = \pm\frac{1}{2\pi}\int_{2\pi+} d\underline{\Omega}_L\,(\underline{\Omega}\bullet\underline{\Omega}_L)\,(\underline{\Omega}'\bullet\underline{\Omega}_L) = \pm\frac{1}{2}\left\{ \frac{1}{2\pi}\int_{4\pi} d\underline{\Omega}_L\,(\underline{\Omega}\bullet\underline{\Omega}_L)\,(\underline{\Omega}'\bullet\underline{\Omega}_L) \right\}. \tag{1c}$$

The integrand depends on three vectors: $\underline{\Omega}$, $\underline{\Omega}'$, $\underline{\Omega}_L$. In order to simplify integration, let us choose the coordinate system where X-Y plane coincides with the plane of vectors $\underline{\Omega}'$ and $\underline{\Omega}$ ($\mu' = \mu = 0$). Therefore,

$$\begin{aligned} \underline{\Omega} &= (\cos\varphi,\ \sin\varphi,\ 0), \\ \underline{\Omega}' &= (\cos\varphi',\ \sin\varphi',\ 0), \end{aligned} \tag{2}$$

$$\underline{\Omega}_L = (\sin\theta_L \cos\varphi_L,\ \sin\theta_L \sin\varphi_L,\ \cos\theta_L).$$

Taking into account Eq. (2) and performing trigonometric transformations, we have

$$(\underline{\Omega}_L \bullet \underline{\Omega}')(\underline{\Omega}_L \bullet \underline{\Omega}) = \sin^2\theta_L \cos(\varphi_L - \varphi)\cos(\varphi_L - \varphi'). \tag{3}$$

Let $\beta \equiv \varphi' - \varphi$, an angle between $\underline{\Omega}$ and $\underline{\Omega}'$, $\beta = \arccos(\underline{\Omega} \bullet \underline{\Omega}')$. Let $\chi \equiv \varphi_L - \varphi'$, and $d\chi = d\varphi_L$. Therefore,

$$\begin{aligned}\Gamma^{\pm} &= \pm\frac{1}{4\pi}\int_{-1}^{1} d\mu_L (1-\mu^2{}_L)\int_0^{2\pi} d\chi \cos(\chi+\beta)\cos(\chi)\\ &= \pm\frac{1}{4\pi}\int_{-1}^{1} d\mu_L (1-\mu^2{}_L)\int_0^{2\pi} d\chi \frac{1}{2}[\cos(\beta)+\cos(2\chi+\beta)]\\ &= \pm\frac{1}{4\pi}\int_{-1}^{1} d\mu_L (1-\mu^2{}_L)\int_0^{2\pi} dy \frac{1}{2}[\cos(\beta)+\cos(y)]\,.\end{aligned} \tag{4}$$

Note, the integrand in Eq. (4) is changing sign two times over the interval $[0;2\pi]$:

$$\cos(y) = -\cos(\beta) \Rightarrow y = \pi \pm \beta.$$

Namely, the integrand is positive over $[0;\pi-\beta]$, negative over $[\pi-\beta;\pi+\beta]$ and again positive over $[\pi+\beta;\ 2\pi]$. Therefore,

$$\begin{aligned}I^{+}(\beta) &\equiv \frac{1}{2}\left\{\int_0^{\pi-\beta}[\cos(\beta)+\cos(y)]dy + \int_{\pi+\beta}^{2\pi}[\cos(\beta)+\cos(y)]dy\right\}\\ &= \int_0^{\pi-\beta}[\cos(\beta)+\cos(y)]dy\\ &= (\pi-\beta)\cos(\beta)+\sin(\beta)\,,\end{aligned} \tag{5a}$$

and

$$\begin{aligned}I^{-}(\beta) &\equiv \frac{1}{2}\int_{\pi-\beta}^{\pi+\beta}[\cos(\beta)+\cos(y)]dy\\ &= \int_{\pi-\beta}^{\pi}[\cos(\beta)+\cos(y)]dy\\ &= \beta\cos(\beta)-\sin(\beta).\end{aligned} \tag{5b}$$

Combining Eq. (4) and (5), we have,

$$\Gamma^{\pm} = \pm\frac{I^{\pm}(\beta)}{4\pi}\int_{-1}^{1} d\mu_L(1-\mu^2{}_L) = \pm\frac{I^{\pm}(\beta)}{3\pi}. \tag{6}$$

Finally, substituting Eq. (6) into Eq. (1), we have

$$\begin{aligned}\Gamma_d(\underline{\Omega}'\to\underline{\Omega}) &= \rho_{L,d}\Gamma_d^-(\underline{\Omega}'\to\underline{\Omega}) + \tau_{L,d}\Gamma_d^+(\underline{\Omega}'\to\underline{\Omega})\\ &= \frac{1}{3\pi}\left\{\rho_{L,d}[-\beta\cos(\beta)+\sin(\beta)] + \tau_{L,d}[(\pi-\beta)\cos(\beta)+\sin(\beta)]\right\}\\ &= \frac{\omega_{L,d}}{3\pi}[\sin(\beta)-\beta\cos(\beta)] + \frac{\tau_{L,d}}{3}\cos(\beta).\end{aligned}$$

Problem 13. Given the direction of incoming, $\underline{\Omega}$, and reflected, $\underline{\Omega}'$, fluxes at the leaf surface ($\|\underline{\Omega}\| = \|\underline{\Omega}'\| = 1$) show that the direction of leaf normals $\underline{n}_L(\mu_L,\varphi_L)$ in the case of specular reflection is given by

$$\mu_L = \frac{|\mu'-\mu|}{\sqrt{2(1-\underline{\Omega}'\bullet\underline{\Omega})}},$$

$$\tan\varphi_L = \frac{\sqrt{1-\mu'^2}\sin\varphi' - \sqrt{1-\mu^2}\sin\varphi}{\sqrt{1-\mu'^2}\cos\varphi' - \sqrt{1-\mu^2}\cos\varphi}.$$

Solution. Consider the geometry of interaction of solar beams with a leaf surface in the case of specular reflection as shown in Fig. (1). Given the incoming, $\underline{\Omega}$, and reflected, $\underline{\Omega}'$, directions, the angle between them is given by $\cos\alpha = \underline{\Omega}\bullet\underline{\Omega}'$. The leaf normal in the case of specular reflection is

$$\underline{n}_L = \frac{\underline{\Omega}-\underline{\Omega}'}{\|\underline{\Omega}-\underline{\Omega}'\|}. \tag{1}$$

The norm $\|\underline{\Omega}-\underline{\Omega}'\|$ can be calculated as follows (cf. Fig. 1(b)):

$$\|\underline{\Omega}-\underline{\Omega}'\| = 2\sin\frac{\alpha}{2} = 2\sqrt{\frac{1-\cos\alpha}{2}} = \sqrt{2(1-\underline{\Omega}\bullet\underline{\Omega}')}. \tag{2}$$

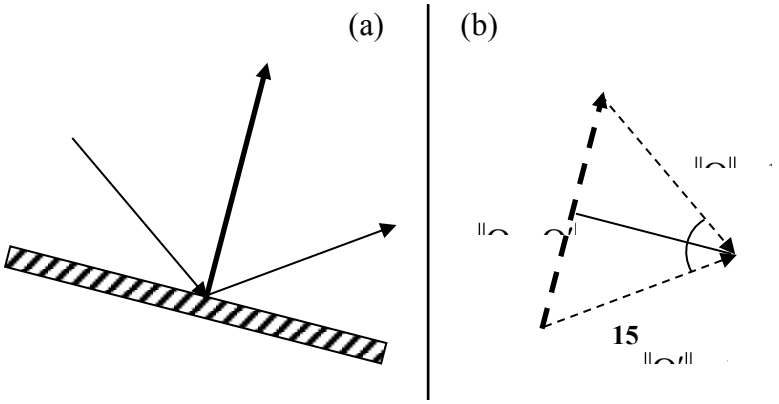

Figure. 1 The geometry of interaction of radiation with leaf. Panel (a) shows direction of leaf surface, leaf normal ($\underline{n}_L$), incoming ($\underline{\Omega}$) and reflected ($\underline{\Omega}'$) beams. Panel (b) is a schematic plot to evaluate the norm of $\|\underline{\Omega}-\underline{\Omega}'\|$.

Let

$$\underline{\Omega} = (\sin\theta\sin\varphi,\ \sin\theta\cos\varphi,\ \cos\theta), \tag{3a}$$

$$\underline{\Omega}' = (\sin\theta'\sin\varphi',\ \sin\theta'\cos\varphi',\ \cos\theta'), \tag{3b}$$

$$\underline{n}_L = (\sin\theta_L\sin\varphi_L,\ \sin\theta_L\cos\varphi_L,\ \cos\theta_L). \tag{3c}$$

Combining Eqs. (1)-(3) we will get formulas for the thee components of vector $\underline{n}_L$, namely,

$$\sin\theta_L\sin\varphi_L = \frac{\sin\theta\sin\varphi - \sin\theta'\sin\varphi'}{\sqrt{2(1-\underline{\Omega}\bullet\underline{\Omega}')}}, \tag{4a}$$

$$\sin\theta_L\cos\varphi_L = \frac{\sin\theta\cos\varphi - \sin\theta'\cos\varphi'}{\sqrt{2(1-\underline{\Omega}\bullet\underline{\Omega}')}}, \tag{4b}$$

$$\cos\theta_L = \frac{\cos\theta - \cos\theta'}{\sqrt{2(1-\underline{\Omega}\bullet\underline{\Omega}')}}. \tag{4c}$$

The Eq. (4c) directly evaluates $\mu_L = \cos\theta_L$. The expression for φ_L can be derived dividing Eq. (4a) by (4b), namely,

$$\tan\varphi_L = \frac{\sin\theta\sin\varphi - \sin\theta'\sin\varphi'}{\sin\theta\cos\varphi - \sin\theta'\cos\varphi'} \equiv \frac{\sqrt{1-\mu^2}\sin\varphi - \sqrt{1-\mu'^2}\sin\varphi'}{\sqrt{1-\mu^2}\cos\varphi - \sqrt{1-\mu'^2}\cos\varphi'}.$$